Aus dem Max von Pettenkofer-Institut für Hygiene und Medizinische Mikrobiologie
Institut der Ludwig-Maximilians-Universität München
Vorstand: Prof. Dr. Sebastian Suerbaum

# Analyse und Charakterisierung des Woronin Körper-Proteins WscA, des Bindeproteins Lah und der Verankerung von Woronin Körpern am Hyphen-Septum im pathogenen Schimmelpilz *Aspergillus fumigatus*.

Dissertation
zum Erwerb des Doktorgrades der Medizin
an der Medizinischen Fakultät der
Ludwig-Maximilians-Universität zu München

vorgelegt von
Yannik Niklas Leonhardt

aus
Kirchheim unter Teck

Jahr
2021

**Mit Genehmigung der Medizinischen Fakultät**
**der Universität München**

| | |
|---|---|
| Berichterstatter: | Prof. Dr. Frank Ebel |
| Mitberichtserstatter: | Prof. Dr. Christina Rieger<br>Prof. Dr. Jürgen Behr<br>PD Dr. Dimitrios Frangoulidis |
| Dekan: | Prof. Dr. med. dent. Reinhard Hickel |
| Tag der mündlichen Prüfung: | 18.03.2021 |

# Eidesstattliche Versicherung

Leonhardt, Yannik

Name, Vorname

Ich erkläre hiermit an Eides statt,

dass ich die vorliegende Dissertation mit dem Thema

Analyse und Charakterisierung des Woronin Körper-Proteins WscA, des Bindeproteins Lah und der Verankerung von Woronin Körpern am Hyphen-Septum im pathogenen Schimmelpilz Aspergillus fumigatus.

selbständig verfasst, mich außer der angegebenen keiner weiteren Hilfsmittel bedient und alle Erkenntnisse, die aus dem Schrifttum ganz oder annähernd übernommen sind, als solche kenntlich gemacht und nach ihrer Herkunft unter Bezeichnung der Fundstelle einzeln nachgewiesen habe.

Ich erkläre des Weiteren, dass die hier vorgelegte Dissertation nicht in gleicher oder in ähnlicher Form bei einer anderen Stelle zur Erlangung eines akademischen Grades eingereicht wurde.

München, 20.04.2021

Ort, Datum

Yannik Leonhardt

Unterschrift Doktorandin/Doktorand

# Inhaltsverzeichnis

# Abkürzungsverzeichnis

| | |
|---|---|
| Abb. | Abbildung |
| ABPA | Allergische bronchopulmonale Aspergillose |
| AIDS | Acquired immunodeficiency syndrome |
| °C | Grad Celsius |
| C-Terminus | Carboxy-Terminus |
| GFP | Grün fluoreszierendes Protein |
| HIV | Human immunodeficiency virus |
| Da | Dalton |
| IgE | Immunglobulin E |
| $\mu$m | Mikrometer |
| nm | Nanometer |
| N-Terminus | Amino-Terminus |
| PCR | Polymerase Chain Reaction |
| PTS-1 | Peroxisomal Targeting Signal |
| RFP | Rot fluoreszierendes Protein |
| WB | Woronin body |
| WSC | Woronin Sorting Complex |

# Publikationsliste

Die folgenden Publikationen sind Teil dieser kumulativen Dissertation:

**Publikation 1:** Leonhardt, Y., Beck, J. and Ebel, F. Functional characterization of the Woronin body protein WscA of the pathogenic mold *Aspergillus fumigatus*. Int J Med Microbiol 306, 165-173 (2016).

**Publikation 2:** Leonhardt, Y., Kakoschke, SC., Wagener, J. and Ebel, F. Lah is a transmembrane protein and requires Spa10 for stable positioning of Woronin bodies at the septal pore of *Aspergillus fumigatus*. Sci Rep. 2017;7:44179.

# 1 Einleitung

Mikroorganismen sind in unserem Umfeld und selbst in unserem eigenen Organismus allgegenwärtig: So sind sie im menschlichen Körper Teil z.B. der normalen Haut-, Mund- oder Darmflora. Andererseits, und das ist für die Medizin seit je von großer Bedeutung, sind sie Auslöser einer Vielzahl an Erkrankungen, die von leichten, nahezu inapparenten Manifestationen bis hin zu schwersten, tödlich verlaufenden Krankheitsbildern führen können. Der menschliche Körper kann mithilfe seines Immunsystems viele Erreger effektiv selbst bekämpfen. Impfungen und die Entwicklung von Antibiotika haben als präventive bzw. therapeutische Maßnahmen enorme Fortschritte gebracht. Aber immer noch zählen Infektionserkrankungen zu den häufigsten Todesursachen weltweit (World Health Organization, 2018). Insbesondere Patienten, die über keine effektive Immunabwehr verfügen – sei es iatrogen beispielsweise im Rahmen von Organtransplantationen und Chemotherapien oder durch Erkrankungen wie etwa HIV/AIDS –, sind zudem bedroht von Mikroorganismen, die für den gesunden Menschen eigentlich keine Bedrohung darstellen. Zu diesen so genannten ”opportunistisch pathogenen” Keimen zählt auch der klinisch relevante Schimmelpilz *Apergillus fumigatus*.

## 1.1 Der filamentöse Pilz *Aspergillus fumigatus*

*A. fumigatus* ist ein Vertreter der Schlauchpilze, den Ascomyceten (Fang and Latgé, 2018). Er ist in der Lage einer großen Bandbreite an Umweltbedingungen zu trotzen, weshalb der Pilz in weiten Teilen der Welt verbreitet vorzufinden ist. Die optimalen Umweltbedingungen liegen bei einer Temperatur von etwa 37°C und einem pH-Wert von 3,7-7,6 – hier kann er bei geeigneten weiteren Umgebungsbedingungen optimal auskeimen und wachsen; jedoch ist *A. fumigatus* ausgesprochen thermostabil und kann bei Temperaturen bis ca. 55°C wachsen und selbst Temperaturen von 70°C trotzen und unter diesen Bedingungen überleben (Latgé, 1999; Kwon-Chung and Sugui, 2013). Das Wachstumsmuster ist filamentös, das heißt in schlauchförmiger Konfiguration, als so genannte ”Hyphe”; die Gesamtheit der Hyphen wird als ”Myzel” bezeichnet. Die Verbreitung über die Distanz geschieht letztlich in Sporenform: An spezialisierten Trägern, den Konidiophoren, entstehen die über die Luft transportfähigen, asexuellen Sporen bzw. Konidien, welche für die Auskeimung an anderer Stelle essentielle Bestandteile enthalten und imstande sind

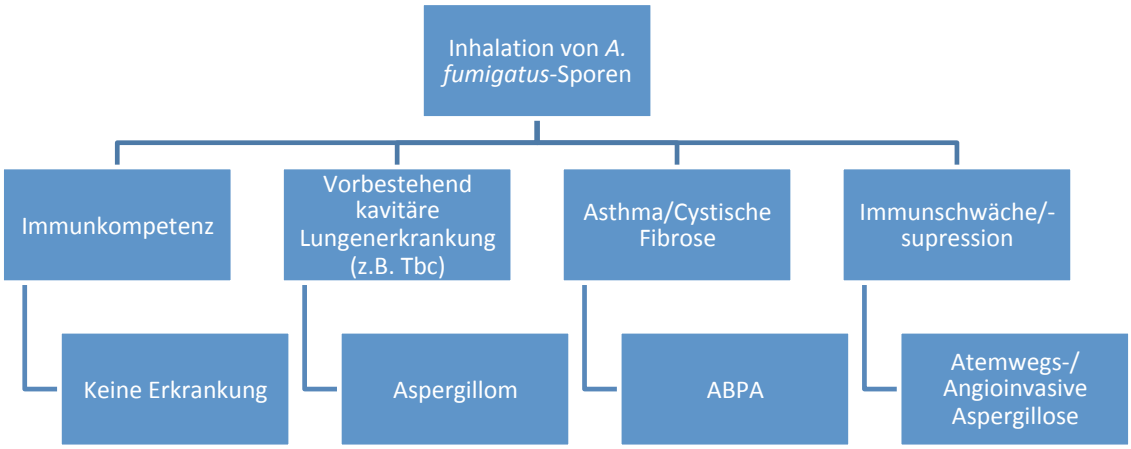


Abbildung 1: Potentielle Auswirkungen inhalierter Sporen von *A. fumigatus* auf den menschlichen Organismus.

verschiedensten Umweltbedingungen zu trotzen (Kwon-Chung and Sugui, 2013).

### 1.1.1 Medizinische Bedeutung

Die Sporen von *A. fumigatus* sind ubiquitär in der Atemluft vorzufinden mit einer Konzentration von durchschnittlich 1-100 Sporen pro Kubikmeter. Mit einem täglichen Atemvolumen von durchschnittlich 10.000-15.000 Liter atmet der Mensch somit jeden Tag potentiell mehrere hundert Sporen ein (Latgé, 1999). Aufgrund ihrer geringen Größe von ca. 2,0-3,0 $\mu$m ist *A. fumigatus* in Sporenform in der Lage bis in die kleinste luftführende Einheit der Lunge, die Alveolen, vorzudringen. Bei Immunkompetenz sind Alveolarmakrophagen im Zusammenspiel mit neutrophilen Granulozyten imstande die Konidien oder bereits aussprossende Hyphen zu bekämpfen und zu eliminieren (Dagenais and Keller, 2009; McCormick et al., 2010).

Abhängig vom Status des Immunsystems und von Vorerkrankungen kann der Kontakt mit *A. fumigatus* unterschiedliche Folgen für den menschlichen Organismus haben. Es werden hierbei im Wesentlichen folgende Krankheitsentitäten unterschieden (vgl. Abb. 1):

Die allergische bronchopulmonale Aspergillose (ABPA) stellt eine chronische allergische Hypersensitivitätsreaktion des Organismus dar. Hierbei handelt es sich um eine chronische Erkrankung der Lunge, die sich intermittierend mit unspezifischen Symptomen wie Atembeschwerden, Husten und sogar Hämoptysen äußern kann. Insbesondere

Menschen mit asthmatischer Grunderkrankung oder Mukoviszidose stellen ein favorisiertes Patientenkollektiv für diese Erkrankung dar (Jumar et al., 2003).

Das Aspergillom bezeichnet eine makroskopisch fassbare, voluminöse Ansammlung von Aspergillushyphen in präformierten Kavitäten: Ein mögliches Beispiel stellen hier die pulmonalen Kavernen dar, wie sie im Rahmen der Tuberkulose entstehen können (Kawamura et al., 2000).

Bei der invasiven Aspergillose kommt es zu einem unkontrollierten Wachstum und Ausbreiten des Schimmelpilzes. Lokal wird dabei eine pulmonale Aspergillose hervorgerufen, jedoch können durch infiltratives Wachstum und über den hämatogenen Weg weitere Organe des Körpers wie etwa das zentrale Nervensystem erreicht werden (McCormick et al., 2010).

Andererseits kann *A. fumigatus*, wenngleich seltener, auch auf nicht-respiratorischem Weg Krankheiten auslösen, so beispielsweise in Auge, Haut oder Gastrointestinaltrakt (Latgé, 1999).

### 1.1.2 Diagnostik und Therapie

Da bei einer manifesten invasiven Aspergillose bei immunsupprimierten Patienten eine hohe Letalität besteht (bis zu 90% bei unbehandelten Patienten z.B. im Rahmen einer Knochenmarktransplantation) (Lin et al., 2001), ist hierbei eine zügige Diagnostik und Therapie essentiell.

Bei klinischem Verdacht auf eine pulmonale Manifestation kann mit Hilfe der Computertomographie nach typischen radiographischen Charakteristika einer pulmonalen Pilzinfektion gesucht werden (Raveendran and Lu, 2018). Ein direkter Erregernachweis kann durch Mikroskopie einer z.B. durch bronchoalveoläre Lavage oder transbronchiale Biopsie gewonnenen Probe erfolgen. Mittels morphologischer Einordnung und Färbeverhalten der Pilzhyphen kann versucht werden den Erreger genauer zu charakterisieren. Auf speziellen Nährböden erfolgt außerdem eine Kultivierung des Pilzes. In der hämatologischen/serologischen Diagnostik können spezifische, pilzeigene Antigene nachgewiesen werden: Hierbei hat sich der Zellwandbestandteil (1,3)-$\beta$-D-Glucan bewährt, welcher bei Nachweis ein Indikator für eine systemische Pilzinfektion darstellt. Speziell für Aspergillus existiert als weiteres, serologisch nachweisbares Antigen das so genannte Galactomannan. Eine weitere Möglichkeit besteht in einer Aspergillus-PCR aus gewonnenem

Patientenmaterial (Ullmann et al., 2018).

Bei klinischem Verdacht und entsprechendem Immunstatus des Patienten wird oftmals bereits frühzeitig eine kalkulierte antimykotische Therapie eingeleitet. Es stehen im Wesentlichen drei verschiedene Substanzklassen zur Verfügung: Amphotericin B führt über eine Steigerung der Permeabilität zu einer Instabilität der Zellmembran des Pilzes. Eine weitere Substanzklasse sind die Triazole mit dem wichtigen Vertreter Voriconazol; diese schränken die Bildung des für die Zellmembran wichtigen Ergosterols ein. Als weitere Möglichkeit bietet sich zur second-line Therapie mit z.B. Caspofungin ein Vertreter der Echinocandine an, welche die Bildung des oben bereits erwähnten (1,3)-$\beta$-D-Glucans als essentiellen Zellwandbestandteil hemmen (Ullmann et al., 2018; Latgé, 1999; Aruanno et al., 2019).

Die Diagnose einer ABPA wird in der Regel über Anamnese und verschiedene Allergie-Tests (z.B. positiver Prick-Test, erhöhtes IgE im Serum) gestellt; die Therapie umfasst unter anderem die Optimierung der Behandlung des oftmals zugrunde liegenden Asthmas sowie ein Absuchen des Patientenumfelds nach potentiellen Quellen für ein erhöhtes Aufkommen von Pilzsporen (Jumar et al., 2003).

Ein Aspergillom kann mit Hilfe von Bildgebung diagnostiziert werden, so z.B. durch ein konventionelles Röntgenbild oder eine computertomographische Aufnahme des Thorax; die definitive Therapie besteht in der chirurgischen Entfernung (Zheng et al., 2018; Latgé, 1999).

## 1.2 Hyphen, Septen und interzelluläre Kommunikation

Nach Auskeimen wachsen filamentöse Ascomyceten als schlauchförmige Hyphe, welche sich in gewissen Abständen verzweigt und somit multidirektional wachsen kann. Hierbei kann bei entsprechenden Bedingungen aus einer einzelnen Spore ein weit verzweigtes, synzytiales Pilzgeflecht entstehen.

Dieses zusammenhängende Hyphengebilde wird in regelmäßigen Abständen durch Septen in kleinere Kompartimente unterteilt. Diese Kompartimente sind jedoch nicht vollständig voneinander isoliert: Zentral in den Septen befindet sich eine Pore mit ca. 50-500 nm Durchmesser, was einen Austausch zwischen den Kompartimenten und sogar einen Transport von kleineren Organellen erlaubt und eine effektivere Verteilung für das Wachstum wichtiger Nährstoffe und Proteine erlaubt (Shatkin and Tatum, 1959; Bleichrodt et al.,

2012).

Jedoch sind diese Septen mit ihren Poren eine potentielle Schwachstelle mit einer Konsequenz für die gesamte Hyphe: Bei einer Schädigung der Zellwand an einer beliebigen Stelle ist prinzipiell die gesamte Hyphe betroffen, da der Zellsubstanzverlust am Ort der Schädigung durch die über die Poren geschaffene interzelluläre Verbindung potentiell jedes Kompartiment betrifft und hierbei die Gefahr eines "Ausblutens" der gesamte Hyphe besteht. Um dies zu verhindern besitzen filamentöse Ascomyceten, und so auch *A. fumigatus*, ein einzigartiges Organell: Die so genannten Woronin bodies (Beck and Ebel, 2013).

## 1.3 Entstehung, Aufbau und Verankerung der Woronin bodies

Bereits 1864 wurden durch den Mykologen Michael Strepanovitch Woronin lichtmikroskopisch sichtbare "kleine Körnchen" in *Ascobolus pulcherrimus* beschrieben, welche sich in der Nähe der Querwände der Pilzhyphen befinden (Woronin, 1864).

Dabei sind die nach ihrem Entdecker benannten Woronin bodies (WBs), wie sich gezeigt hat, Organellen *filamentöser* Ascomyceten: WBs sind etwa in der Hefe-Form der zu den Ascomyceten gehörigen dimorphen Pilze *Blastomyces dermatidis* oder *Histoplasma capsulatum* nicht nachweisbar, in der filamentösen Hyphen-Form jedoch schon (Garrison et al., 1970).

Über einhundert Jahre nach ihrer Entdeckung wurde in *Neurospora crassa* gezeigt, dass diese einzigartigen Organellen, wie bereits vorher schon vermutet, im Falle einer Zellwandschädigung die septalen Poren abdichten können (Trinci and Collinge, 1974). WBs dienen somit der Erhaltung der strukturellen Integrität des Pilzfilaments im Falle einer Zellwandschädigung und verhindern letztlich einen übermäßigen Verlust von Cytoplasma (Jedd and Chua, 2000; Tenney et al., 2000). In mehreren Arbeiten konnte gezeigt werden, dass WBs eine wichtige Rolle in der Stressresistenz und Virulenz spielen, so etwa in *Magnaporthe grisea* (Soundararajan et al., 2004), *Arthrobotrys oligospora* (Liang et al., 2017) und auch in *A. fumigatus* (Beck et al., 2013). In *A. fumigatus* konnte in Abwesenheit von WBs ferner eine erhöhte Sensitivität gegenüber das Antimykotikum Caspofungin nachgewiesen werden (Dichtl et al., 2015).

Die genauen Bestandteile, ihr Zusammenspiel und die Biogenese der WBs sind nach wie vor nicht vollständig geklärt und sind Bestandteil laufender Forschung. WBs sind in

ihrem Durchmesser etwas größer als die jeweiligen septalen Poren und bestehen elektronenmikroskopisch aus einem dichten, osmophilen Kern, welcher von einer Membran umgeben ist (Collinge and Markham, 1985; Markham and Collinge, 1987). Durch biochemische Aufreinigungen konnte erstmals in *N. crassa* das Protein HEX-1 als ein Hauptbestandteil identifiziert werden. Dieses Protein besitzt ein C-terminales PTS-1-Motiv, welches einen Import in Peroxisomen zur Folge hat. In den Peroxisomen aggregiert HEX-1 in größeren kristallinen Formationen; letztlich schnüren sich aus den Peroxisomen dicht mit diesem Protein gefüllte, reife WBs ab (Jedd and Chua, 2000). HEX-1 ist für die Entstehung von WBs essentiell, denn eine Deletion des entsprechenden Gens führt zu einem vollkommenen Verlust von WBs (Jedd and Chua, 2000; Tenney et al., 2000). Ein entsprechendes Homolog (HexA) mit äquivalenten Eigenschaften wurde in *A. fumigatus* bereits beschrieben und charakterisiert (Beck and Ebel, 2013).

Als weiterer Bestandteil wurde in *N. crassa* das Membranprotein WSC (woronin sorting complex) identifiziert (Liu et al., 2008). Auch dieses wird an die Peroxisomen rekrutiert, wobei hier der Targeting-Mechanismus unbekannt ist. Im Rahmen dieser Arbeit wurde das entsprechendes Homolog in *A. fumigatus* (WscA) analysiert und charakterisiert (Leonhardt et al., 2016).

Die reifen WBs sind in den meisten filamentösen Pilzen prinzipiell frei im Zytoplasma verteilt; um ihrer Funktion jedoch suffizient nachzukommen, erscheint es jedoch naheliegend, dass einige WBs porennah verankert sind, so dass sie die Pore im Falle einer Zellschädigung schnell verschließen können (Beck and Ebel, 2013). Tatsächlich lassen sich mikroskopisch stets WBs in Septumnähe nachweisen: Ein typisches Verteilungsmuster von WBs in *A. fumigatus* zeigt Abb. 2.

Experimente, in denen WBs in Septumnähe von ihrer Position mit Hilfe einer Laser-Pinzette von der Pore distanziert wurden, haben gezeigt, dass die entsprechenden WBs nach kurzer Zeit wieder in ihre Position zurückkehren (Berns et al., 1992): Einige WBs zeigen also eine flexible, aber insgesamt feste Verankerung am Septum. Ein filamentöser Charakter dieser Verbindungsstruktur konnte elektronenmikroskopisch in *A. nidulans* gezeigt werden (Momany et al., 2002).

Für die Verankerung am Septum wurde in *A. fumigatus* mittlerweile ein riesiges Protein mit ca. 500.000 Da identifiziert, das so genannte *leashin*- bzw. Lah-Protein. Dabei ist der C-Terminus von Lah mit dem Septum verankert, wohingegen der N-Terminus mit

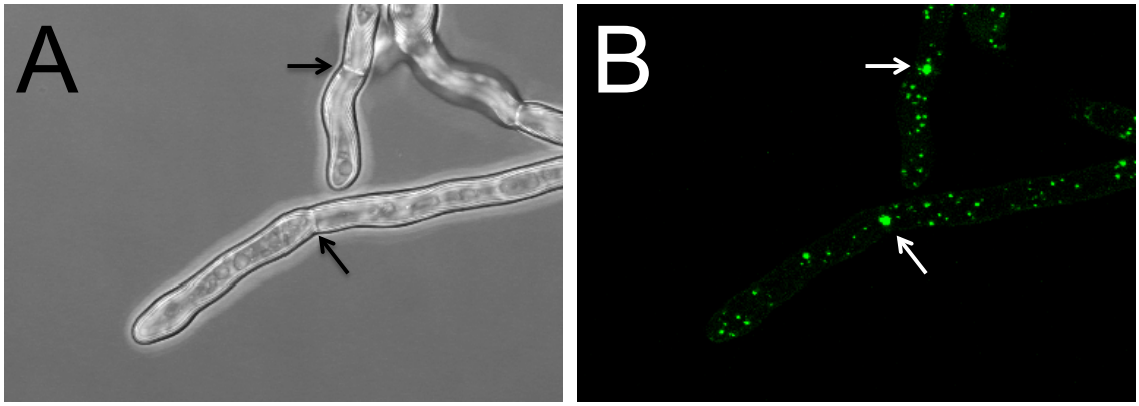


Abbildung 2: Konfokalmikroskopische Aufnahme von Hyphen des AfS35, welcher ein LahN-GFP-Konstrukt exprimiert. (A) zeigt die Durchlichtaufnahme, die Pfeile markieren zwei reife Septen. (B) Fluoreszenzmikroskopische Aufnahme derselben Hyphen. Durch das LahN-GFP-Konstrukt werden die Woronin bodies markiert und sichtbar gemacht macht. Die Pfeile markieren die Septen aus Bild (A).

dem WB interagiert (Beck et al., 2013).

Der genaue Verankerungsmechanismus bzw. die entsprechenden Interaktionspartner an Septum und WB waren sowohl N- als auch C-terminal zu Beginn der Arbeit in *A. fumigatus* noch nicht charakterisiert. Für die Interaktion zwischen *leashin*-Protein und WB wurde in *N. crassa* zwar das WSC-Protein, das Homolog von WscA, identifiziert (Ng et al., 2009). Die Übertragbarkeit dieses Modells auf *A. fumigatus* ist jedoch zweifelhaft, denn es unterscheiden sich bereits auf mikroskopischer Ebene die WBs in *N. crassa* von denen der meisten anderen Pezizomycotina: So sind in *N. crassa* die WBs ausschließlich an der lateralen Zellwand verankert und nicht am Septum bzw. frei im Zytoplasma befindlich. Zudem unterscheiden sich die Bestandteile des Verankerungskomplexes deutlich: So interagiert in *N. crassa* der C-Terminus des WSC mit LAH-1 (das funktionelle Lah-Homolog) (Ng et al., 2009), jedoch sind in den meisten Pezizomycotina, so auch in *A. fumigatus*, weder das LAH-1 noch das C-terminale Ende von WSC konserviert (vgl. Abb. 3) (Leonhardt et al., 2016; Beck et al., 2013).

Für die Verankerung am Septum wurden bereits die 1000 C-terminalen Aminosäuren von Lah als ausreichend identifiziert (Beck et al., 2013). Es wurde in *N. crassa* sowie *A. nidulans* in der Vergangenheit bereits eine Gruppe von Proteinen beschrieben und charakterisiert, die – ähnlich den WBs bzw. dem C-Terminus von Lah in *A. fumigatus* – mit den Zellsepten assoziiert und dort lokalisiert zu finden sind (septum-pore-associated proteins, *SPA*) (Shen et al., 2014; Lai et al., 2012). Eine Analyse bezüglich einer potentiellen Interaktion zwischen Lah-Protein und Spa-Proteinen bzw. eine genauere Charakterisierung des Verankerungsmechanismus des Lah-Proteins am Septum existierte zu Beginn

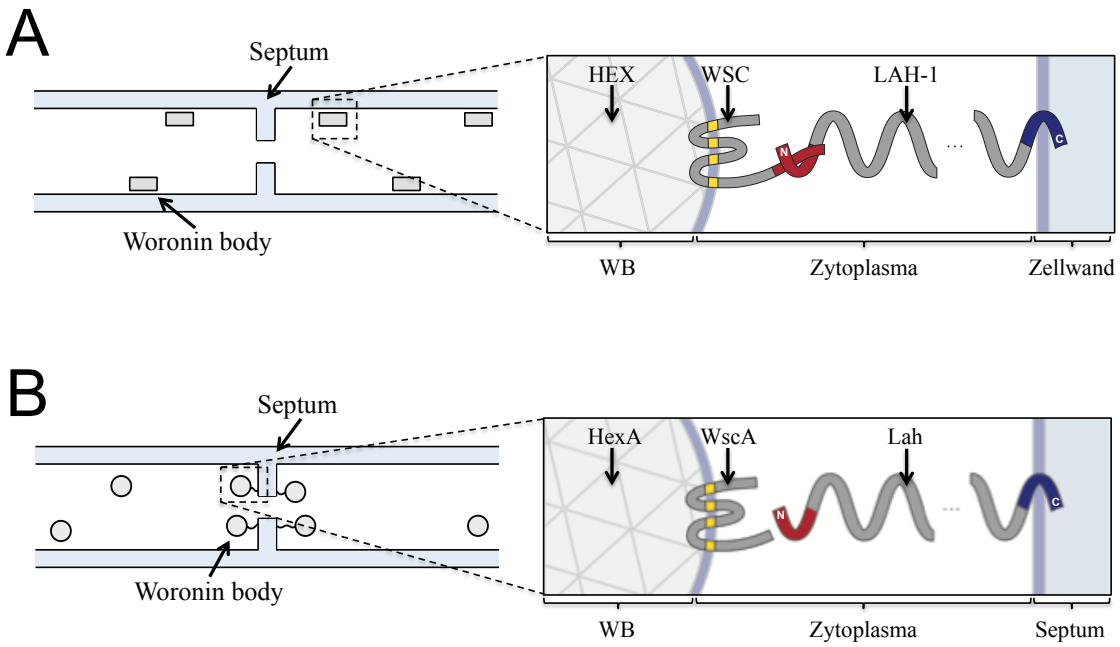


Abbildung 3: Schematische Darstellung der an der Verankerung von Woronin bodies beteiligten Bestandteile in (A) *N. crassa* und (B) *A. fumigatus*.

der Arbeit jedoch nicht.

Wie oben beschrieben ist *A. fumigatus* ein medizinisch bedeutsamer Erreger, welcher aufgrund seiner Resistenz gegenüber widrigen Umweltbedingungen weit verbreitet und überlebensfähig ist. WBs sind ein wichtiger Bestandteil dieser Stressresistenz von *A. fumigatus*. Um diesen Apparat besser verstehen zu können ist eine grundlegende Erforschung und Charakterisierung der WBs und des Verankerungsmechanismus am Septum essentiell. In dieser Arbeit wurde in zwei Publikationen einerseits eine funktionelle Charakterisierung des WscA-Proteins, andererseits eine genaue Analyse des C-Terminus von Lah vorgenommen sowie ein potentieller Interaktionspartner am Septum, das septum-pore-associated protein Spa10, identifiziert.

## 1.4 Erklärung zum Eigenanteil an den Publikationen

In beiden vorliegenden Publikationen ist der Autor dieser Dissertation der Erstautor, wobei in Leonhardt et al., 2017 eine geteilte Erstautorschaft vorliegt.

**Publikation 1:** Leonhardt, Y., Beck, J. and Ebel, F. Functional characterization of the Woronin body protein WscA of the pathogenic mold *Aspergillus fumigatus*. Int J Med Microbiol 306, 165-173 (2016).

Alle Experimente dieser Publikation wurden durch Yannik Leonhardt durchgeführt. Dies umfasst die Generierung der jeweiligen Reporter-Konstrukte für WscA (wscA-gfp, gfp-wscA), ihrer Expression in der für diese Publikation erzeugten wscA-Deletionsmutante sowie im Wildtyp, die (fluoreszenz-)mikroskopische Analyse sowie statistische Auswertung; im Einzelnen: Mikroskopie und statistische Auswertung der räumlichen Verteilung von WBs in der Δ*wscA*-Mutante vor und nach Komplementierungsversuchen (Figure 1a-c), die Analyse bezüglich Kolokalisation von HexA und Peroxisomen in der Δ*wscA*-Mutante (Figure 2a-d), die hochaufgelöste mikroskopische Darstellung von HexA in Peroxisomen im zeitlichen Verlauf (Figure 3a-f), die direkte Darstellung von WscA mittels GFP-Reporterkonstrukten (Figure 4a-h), Analyse und Visualisierung der Anfälligkeit der WB-Biogenese durch N-terminale Modifikation von WscA mittels Fluoreszenzmikroskopie und Immunoblot-Analyse (Figure 5) sowie die Expression und Fluoreszenzmikroskopie von HexA-GFP in der Δ*wscA*-Mutante (Figure 6).

Durch Julia Beck wurden die bereits generierte Mutante Δ*hexA* und weitere Reporter-Konstrukte (rfp-PTS1, hexA-gfp, gfp-hexA) zur Verfügung gestellt (Beck and Ebel, 2013; Beck et al., 2013).

In Zusammenarbeit mit dem Letztautor Frank Ebel wurden die jeweiligen Experimente konzipiert, ausgewertet sowie das Manuskript verfasst.

**Publikation 2:** Leonhardt, Y., Kakoschke, SC., Wagener, J. and Ebel, F. Lah is a transmembrane protein and requires Spa10 for stable positioning of Woronin bodies at the septal pore of *Aspergillus fumigatus*. Sci Rep. 2017;7:44179.

Die beiden Erstautoren dieser Publikation hatten einen etwa gleichen Anteil an den Ex-

perimenten. Durch Sara C. Kakoschke erfolgte die Klonierung und Charakterisierung des LahC-Proteins (Figure 1a-c), die Charakterisierung und Klonierung von $LahC_{TM}$ (Figure 2a-f) sowie die Darstellung des Recruitments von LahC während der Septumformation (Figure 3) und die Charakterisierung von LahC in der Δ*roh4*-Mutante (Figure 5a und b).

Durch Yannik Leonhardt wurde das Verhalten der WBs während der Septenentstehung beleuchtet (Figure 4), die Erzeugung und Analyse der Δ*spa10*-Mutante vorgenommen, das Verhalten von WBs und LahC in dieser Mutante charakterisiert (Figure 6 und 7), die Δ*spa10*-Mutante mittels spa10-rfp-Konstrukt komplementiert (Figure 8) sowie das hypothetische Modell zur Rekrutierung von Lah und WBs während der Septumformation erstellt (Figure 9).

Johannes Wagener hat die Δ*rho4*-Mutante zur Verfügung gestellt (Dichtl et al., 2012). In Zusammenarbeit mit dem Letztautor Frank Ebel wurden die jeweiligen Experimente konzipiert, ausgewertet sowie das Manuskript verfasst.

# 2 Zusammenfassung

*A. fumigatus* ist ein klinisch relevanter Krankheitserreger, welcher verschiedene Krankheitsentitäten hervorrufen und insbesondere bei immunkompromittierten Patienten potentiell letal verlaufende systemische Infektionen auslösen kann.

Der filamentöse Pilz bildet Hyphen, welche durch Septen in verschiedene Kompartimente unterteilt werden. Durch eine zentrale Pore in den Septen bleiben die Kompartimente in Verbindung und können Moleküle und kleinere Organellen austauschen. Es besteht dadurch aber die Gefahr, dass das Pilzgeflecht bei lediglich lokalem Schaden durch die geschaffene interzelluläre Verbindung in seiner Gesamtheit gefährdet ist. Um dieser Gefahr zu entgehen, können die Poren des entsprechenden Kompartiments bei einem Zellwandschaden verschlossen werden. Dies ermöglichen Woronin bodies (WBs), sphärisch geformte, pilzspezifische Organellen mit für diese Aufgabe entsprechender Größe und porennaher Positionierung am Septum. Es sind drei Proteine bekannt, die essentiell für die Entstehung und feste Positionierung von WBs am Septum sind: (i) Das HexA-Protein, welches eine kristallartige Struktur innerhalb der WB-Matrix bildet; (ii) das Protein WscA, welches sich in der Peroxisomen- und WB-Membran befindet; (iii) das Lah-Protein, ein Polypeptid aus 5538 Aminosäuren, welches WB mit dem Septum verbindet. Die vorliegenden Publikationen befassen sich mit der Charakterisierung des WscA-Proteins sowie der Verankerung des Lah-Proteins am Septum.

Das Lah-Protein ist mit seinem C-Terminus am Septum verankert, wobei bereits gezeigt werden konnte, dass dafür die 1000 C-terminalen Aminosäuren ausreichend sind (Beck et al., 2013). Diese 1000 Aminosäuren des C-Terminus von Lah (LahC) wurden mit Hilfe von transmembrane prediction tools (TMpred, Phobius) auf potentielle Transmembrandomänen untersucht, welche als Orientierung für weitere Verkürzungen des Proteins dienten. Diese Verkürzungen wurden N-terminal mit einem GFP-Tag versehen, im Pilz exprimiert und mikroskopiert. Die minimale, noch korrekt am Septum lokalisierende Verkürzung von LahC besteht aus den terminalen 288 Aminosäuren ($LahC_{288}$), welche eine TM-Domäne und einen C-terminalen extrazellulären Rest besitzt. Diese beiden Elemente sind essentiell für die korrekte Positionierung am Septum: Ohne die Transmembrandomäne findet sich das Fusionsprotein diffus im Zytosol verteilt und ohne die extrazelluläre Komponente erfolgt eine Anreicherung des GFP-$LahC_{288}$ in den Vakuolen des Pilzes.

Außerdem wurde auch der Prozess der Septenentstehung näher beleuchtet: Es konnte

sowohl für das LahC (mittels GFP-LahC) als auch für die WBs (mittels LahN-GFP) gezeigt werden, dass eine Rekrutierung an die Stelle eines entstehenden Septums bzw. die entsprechende Stelle der lateralen Zellwand stattfindet, bevor das Septum an sich lichtmikroskopisch überhaupt sichtbar war. In einer Δ*rho4*-Mutante, welche eine stark verminderte Septenbildung zeigt, konnte beobachtet werden, dass WBs im Vergleich zum Wildtyp vermehrt punktuell an der lateralen Zellwand verharren, möglicherweise ein Hinweis auf hier befindliche Verankerungsstellen für das Lah-Protein an potentiellen Septierungsstellen, wobei die Septierung aufgrund der Rho4-Deletion nicht weiter zur Ausprägung kommt.

In der Suche nach einem Interaktionspartner oder Rezeptor für das Lah-Protein am reifen Septum wurde als potentieller Kandidat das Protein Spa10 identifiziert. Spa10 ist am reifen Septum lokalisiert, zeigt im Gegensatz zum Lah-Protein bzw. den WBs aber keine frühe Assoziation zum Entstehungsort eines Septums; jedoch zeigt sich in Abwesenheit von Spa10 in einer entsprechenden Deletionsmutante, dass WBs zwar am entstehenden Septum wie im Wildtyp lokalisieren, jedoch am reifen Septum nicht oder nur transient verankert sind. Spa10 scheint eine Art stabilisierende Funktion für die Verankerung der WBs bzw. des Lah-Proteins am Septum zu erfüllen.

Des Weiteren wurde eine funktionelle Analyse des WscA-Proteins vorgenommen. Zunächst wurde eine Δ*wscA*-Mutante erzeugt und die Verteilung und Lokalisation des WB-Strukturproteins HexA untersucht. In Abwesenheit von WscA zeigt sich ein GFP-HexA Fusionsprotein überwiegend in Peroxisomen und nicht, wie im Wildtyp, in für WBs typischer Lokalisation am Septum und im Zytosol verteilt; ohne WscA kann der Pilz also nicht mehr adäquat WBs bilden. In hochauflösenden fluoreszenzmikroskopischen Bildern konnte außerdem gezeigt werden, dass GFP-HexA in den Peroxisomen der WscA-Deletionsmutante an bestimmten Stellen verdichtet aggregiert und eine Donut-ähnliche Form bildet.

Im nächsten Schritt wurden GFP-Fusionskonstrukte mit WscA selbst erzeugt und die Verteilung und Lokalisation der Fusionsproteine untersucht. WscA-GFP (C-terminale Fusion) lässt sich einerseits in WBs in eindeutiger bzw. üblicher Positionierung am Septum nachweisen, eine überwiegende Menge des WscA-GFP befand sich jedoch in der Membran der Peroxisomen. Eine vollständige Komplementierung der WscA-Deletionsmutante mittels WscA-GFP war nicht möglich, da nach Expression des Konstrukts in der Deleti-

onsmutante im Vergleich zum Wildtyp deutlich weniger WBs am Septum nachgewiesen werden konnten (Reduktion auf ca. 46%); eine C-terminale Modifikation scheint also eine WB-Positionierung am Septum zu erschweren. Eine Fusion von GFP an den N-Terminus von WscA hatte noch einen deutlicheren Effekt: Hier waren kaum WBs an den Zellsepten nachweisbar; eine Modifikation des N-Terminus beeinträchtigt also die Funktion des WscA und die Bildung von WBs.

WscA scheint also einerseits essentiell für die Entstehung von WBs zu sein und andererseits sehr sensibel auf (insbesondere N-terminale) Modifikation zu reagieren mit Konsequenz auf die Verankerung von WBs am Septum.

WBs sind ein wichtiger Bestandteil für die Stressresistenz von *A. fumigatus*. Essentielle Bestandteile für die Verankerung und Biogenese von WBs konnten in den vorliegenden Publikationen näher charakterisiert bzw. identifiziert werden. Ein abschließendes, vollständiges Modell liegt nach wie vor nicht vor und ist Aufgabe weiterer Forschung.

# 3 Summary

*A. fumigatus* is a major fungal pathogen causing various diseases and potentially life-threatening infections in particular in immunocompromised patients.

The filamentous mold is compartmentalised by septa which have central pores that allow an exchange of molecules and organelles between the compartments. This intercellular connection is a potential risk for the whole hypha if the cell wall is damaged. To limit cytoplasmic bleeding in case of cell wall damage the septal pores are being plugged by specialised organelles called 'Woronin bodies' (WBs). WBs are spherical structures that are, in order to fulfil their function, localised at the septa in the vicinity of the central pores. Three proteins have been identified to be essential for the biogenesis and linkage to the septum: (i) the HexA-Protein, which forms a crystalline structure in the WB-Matrix; (ii) the WscA-Protein, which is located in the membrane of the peroxisomes and WBs; (iii) the Lah protein, a polypeptide consisting of 5538 amino acids, which connects WBs to the septum. The presented publications address the characterisation of WscA and the anchoring of the Lah-protein to the septum.

With its C-terminus Lah is connected to the septum. In a previous study the 1000 C-terminal amino acids were shown to be sufficient for a correct localisation at the septum (Beck et al., 2013). The C-terminal 1000 amino acids (LahC) were analysed using transmembrane prediction tools (TMpred, Phobius). Those transmembrane domains served as reference points for further truncations of the protein. The truncated proteins were tagged with an N-terminal GFP and analysed by fluorescence microscopy. The smallest fragment of LahC with the correct localisation at the septum consists of the C-terminal 288 amino acids ($LahC_{288}$), which contain one TM-domain and a C-terminal extracellular domain. These elements are essential for the correct localisation at the septum: without the transmembrane segment the fusion protein is distributed diffusely in the cytosol; without the extracellular domain the truncated protein accumulates in vacuoles.

The process of septation was furthermore analysed in wild type strains expressing a GFP-LahC fusion protein as well as in strains expressing a LahN-GFP fusion protein (which tags WBs). LahC and WBs respectively were recruited to the site of an emerging septum, when the septum itself was not visible yet. In a Δ*rho4* mutant, which shows a severe defect in septation, WBs were found to remain at certain points at the lateral cell wall potentially indicating anchoring points for the WBs or Lah at possible septation sites

that fail to manifest due to deletion of Rho4.

In search for a suitable interaction partner or receptor for the Lah protein at the septum the septum pore associated protein Spa10 was identified as promising candidate. Spa10 is located at the mature septum, but does not show the recruitment to the early site of septation like LahC/WBs; however in Δ*spa10* mutants WBs are only transiently, if at all, anchored to the mature septum. Spa10 seems to have some kind of a stabilising function for the anchoring mechanism of LahC/WBs.

In further studies we characterised the membrane protein WscA. In a first step a Δ*wscA* mutant was generated to analyse the effect on the biogenesis and distribution of WBs. In this mutant HexA (visualised by an N-terminal GFP tag) is largely found in peroxisomes, not at WB-typical localisations (septum and cytosol); this suggests that WBs fail to be formed in absence of WscA. High-resolution fluorescence microscopy images revealed, that in the deletion mutant GFP-HexA aggregates at certain points in the peroxisomes in the form of donut-like structures.

In a next step we analysed N- and C-terminal fusion constructs of WscA regarding localisation und spatial distribution. WscA-GFP (C-terminal fusion) accumulates in peroxisomal membranes as well as in spot-like structures in for WBs typical localisations like the cytosol and near the septum. A full functional complementation of the Δ*wscA* mutant using WscA-GFP could not be achieved: in contrast to the wild type the number of WBs in the direct vicinity of the septal pores was reduced to approx. 46%; a C-terminal modification seems to impair the efficient positioning of the WBs at the septum. The impact of an N-terminal modification is even more severe: in an attempt to complement the mutant with GFP-WscA almost no WBs were located at the septa. WscA seems to be essential for the biogenesis of WBs and reacts highly sensitive to C- and especially N-terminal modifications with direct consequences for the anchoring of WBs to the septum.

WBs are important for the stress resistance of *A. fumigatus*. In the presented publications essential components for the biogenesis and the anchoring mechanism of WBs were identified and characterised; to form a complete and comprehensive model of this unique structure further research is required to define the various components and their interactions in more detail.

# 4 Publikationen

**4.1** Leonhardt, Y., Beck, J. and Ebel, F. Functional characterization of the Woronin body protein WscA of the pathogenic mold *Aspergillus fumigatus*. Int J Med Microbiol 306, 165-173 (2016).

Seite 19 - 27

International Journal of Medical Microbiology 306 (2016) 165–173

Contents lists available at ScienceDirect

International Journal of Medical Microbiology

journal homepage: www.elsevier.com/locate/ijmm

# Functional characterization of the Woronin body protein WscA of the pathogenic mold *Aspergillus fumigatus*

Yannik Leonhardt[a], Julia Beck[a], Frank Ebel[a,b,c,*]

[a] *Max-von-Pettenkofer-Institute, LMU, Munich, Germany*
[b] *Institute for Infectious Diseases and Zoonoses, LMU, Munich, Germany*
[c] *German Center for Infection Research (DZIF), Munich, Germany*

ARTICLE INFO

*Article history:*
Received 6 February 2016
Received in revised form 14 March 2016
Accepted 17 March 2016

*Keywords:*
Woronin body
Septum
Aspergillus fumigatus
WscA
HexA
Peroxisome

ABSTRACT

Woronin bodies are fungal-specific organelles that seal damaged hyphal compartments and thereby contribute to the stress resistance and virulence of filamentous fungi. In this study, we have characterized the *Aspergillus fumigatus* Woronin body protein WscA. WscA is homologous to *Neurospora crassa* WSC, a protein that was shown to be important for biogenesis, segregation and positioning of Woronin bodies. WscA and WSC both belong to the Mpv17/PMP22 family of peroxisomal membrane proteins. An *A. fumigatus* Δ*wscA* mutant is unable to form Woronin bodies, and HexA, the protein that forms the crystal-like core of Woronin bodies, accumulates in large peroxisomes instead. The Δ*wscA* mutant showed no defect in segregation of HexA containing organelles, as has been reported for the corresponding *N. crassa* mutant. In the peroxisomes of the *A. fumigatus* mutant, HexA assembles into compact, donut-shaped structures. Experiments with GFP fusion proteins revealed that WscA function is highly sensitive to these modifications, in particular to an N-terminal fusion of GFP. In *N. crassa*, WSC was shown to be essentially required for Woronin body positioning, but the respective domain is not conserved in most other *Pezizomycotina*, including *A. fumigatus*. We have recently found evidence that HexA may have a direct role in WB positioning, since a HexA-GFP fusion protein, lacking a functional PTS1 motif, is efficiently recruited to the septal pore. In the current study we show that this targeting of HexA-GFP is independent of WscA.


## 1. Introduction

*Aspergillus fumigatus* is a major fungal pathogen causing life-threatening infections in immunocompromised patients and certain animals, in particular birds (Tell, 2005; McCormick et al., 2010). A main focus in the research on *A. fumigatus* is the identification and characterization of molecules and structures that contribute to the remarkable robustness of this pathogen (Tekaia and Latgé, 2005) and may therefore represent suitable targets for new therapeutic approaches.

Woronin bodies (WB) are specialized organelles that are exclusively found in filamentous fungi (Woronin, 1864; Maruyama and Kitamoto, 2013). They seal damaged compartments and thereby protect wounded hyphae from extensive loss of cytoplasm (Collinge and Markham, 1985; Tenney et al., 2000; Jedd and Chua, 2000). An *A. fumigatus* mutant lacking WBs is attenuated in virulence and shows a higher sensitivity to certain antifungals (Beck et al., 2013a; Dichtl et al., 2015). Apart from this emergency function, WBs represent an important structural element of intact hyphae that can separate compartments to allow heterogeneity and differentiation of specialized cells (Bleichrodt et al., 2012).

In the model fungus *Neurospora crassa*, two major and essential WB proteins, HEX and WSC, have been identified. Both are initially recruited to peroxisomes from which WB are derived. The HEX protein is targeted to peroxisomes by its C-terminal PTS1 motif. After import into the organelle, HEX proteins assemble into large crystal-like structures that fill the internal space of mature WBs (Jedd and Chua, 2000). The peroxisomal targeting of the WSC protein is mediated by a so far unknown mechanism. In the peroxisomal membrane, WSC self-assembles into detergent-resistant oligomers that become enriched at certain surface areas, where it interacts with HEX to initiate WB formation (Liu et al., 2008).

WBs serve the same purpose in all *Pezizomycotina*, but two distinct patterns exist for their positioning: In the *Neurospora*/*Sordaria* clade all WBs are tethered to the lateral hyphal cell wall, whereas in most other *Pezizomycotina* WBs are anchored at septal pores and additionally found free in the cytoplasm (Momany et al., 2002). This

* Corresponding author at: Institute for Infectious Diseases and Zoonoses, LMU, Munich, Germany.
*E-mail address:* frank.ebel@lmu.de (F. Ebel).

http://dx.doi.org/10.1016/j.ijmm.2016.03.008
1438-4221/

difference in WB positioning is also reflected at the protein level. The most prominent example is the tethering protein: LAH1 in *N. crassa* and Lah in *A. fumigatus*. Both are similar in size, but share no homology. WSC is the second protein that is essential for the positioning of WBs in *N. crassa*. Its C-terminus extends into the cytoplasm and the terminal 71 amino acids interact with LAH-1, which physically links WBs to the lateral cell wall (Liu et al., 2008; Ng et al., 2009). In most *Pezizomycotina,* neither LAH-1 nor the C-terminal motif of WSC are conserved, it therefore appears that the WB positioning machinery found in *Neurospora* and *Sordaria* evolved from the apparatus found in most other *Pezizomycotina* to meet the specific requirements in this fungal clade (Ng et al., 2009; Beck et al., 2013).

In this study, we have characterized WscA, the WSC homolog in *A. fumigatus*. WscA and WSC are homologous, except for the C-terminal 71 amino acids of WSC. Using a *wsc*A deletion mutant and GFP-fusion proteins we have analysed the biological function of WscA in *A. fumigatus*. Our data demonstrate that WscA, like WSC, plays an important role in WB biogenesis, whereas both proteins have apparently diverse functions in WB positioning and inheritance.

## 2. Results

The *A. fumigatus* gene AFUA_2G17080 encodes a protein of 239 amino acids sharing 63.4% identity with *N. crassa* WSC (XP_011393946). Based on this homology, it was designated WscA (Beck et al., 2013). WSC and WscA have a similar structure consisting of four membrane spanning regions, connected by three short loops, and two terminal domains that extend into the cytoplasmic space (Suppl. Fig. 1) with the two terminal domains being the most variable parts.

To study the function of WscA, we deleted the corresponding gene and subsequently complemented the mutant by ectopic insertion of *wsc*A under the control of the constitutive *gpd*A promoter. The strategy and the genetic verification of the constructs are shown in Suppl. Fig. 2. Growth and colony morphology of the mutant strain are normal. Like the Δ*hex*A mutant, Δ*wsc*A showed an increased sensitivity to the cell wall stressor Calcofluor white, but this phenotype was less pronounced than that of the Δ*hex*A mutant (Suppl. Fig. 3). Under standard growth conditions, the Δ*wsc*A mutant showed no signs of cytoplasmic bleeding or tip lysis (data not shown).

### 2.1. Positioning of WBs at the septal pore depends on WscA

Immunofluorescence analysis of Δ*wscA* hyphae revealed HexA assemblies in the cytosol, but not at septal pores (Fig. 1B and C), whereas re-introduction of the *wsc*A gene fully restored the wild type phenotype with WBs in close proximity to the septal pores. This is also evident from a quantitative analysis shown in Fig. 1A. In the parental strain AfS35 87% of all septa were associated with WBs, whereas in the Δ*wsc*A mutant 93% of septa lacked HexA assemblies. In the remaining 7%, spot-like HexA structures were found in proximity to septal pores, but further experiments using time lapsed microscopy revealed that this represents only random localizations (Video 1).

### 2.2. Localisation of HexA in the Δ*wscA* mutant

After expression in the Δ*wscA* mutant, a fusion of GFP to the N-terminus of HexA (GFP-HexA) showed the same spatial distribution in HexA assemblies as observed for HexA using immunofluorescence (data not shown). Live cell imaging confirmed that all HexA structures were motile and not anchored at septal pores (Video 1).

In the *N. crassa wsc* mutant, apical compartments contain seven times more HEX aggregates than apical compartments of wild type hyphae. Moreover, subapical compartments were in contrast to those in wild type hyphae devoid of HEX aggregates (Liu et al., 2008). This striking defect in segregation was not observed for the Δ*wscA* mutant (Fig. 2 and data not shown).

The *N. crassa wsc* mutant lacks WBs and HEX assemblies reside in large peroxisomes instead, wherein they move randomly (Liu et al., 2008). In the Δ*wscA* mutant, most GFP-HexA is found in peroxisomes of variable size (Fig. 2A–C). Only few GFP-HexA positive organelles were observed that lacked the peroxisomal marker RFP-PTS1 and thereby and in their size resembled mature WBs, but none of them was anchored at septal pores (Fig. 2, arrowheads). RFP-PTS1-positive peroxisomes without GFP-HexA were not observed (Fig. 2C).

In live cell imaging, a variable morphology was evident for some of the large peroxisomes that were filled up with GFP-HexA (Video 1). This is remarkable, since Hex proteins usually assemble into rigid crystal-like structures (Jedd and Chua, 2000). The presence of soluble GFP-HexA molecules in the peroxisomal lumen is also suggested by their co-localization with RFP-PTS1, a protein that is normally excluded from HexA assemblies in WBs.

GFP-HexA fluorescence in the larger peroxisomes was much stronger than in the smaller assemblies. Reducing the gain used to record the GFP signals revealed substructures or more precisely the presence of one highly fluorescent, donut-shaped structure per peroxisome. The intense fluorescence suggests that GFP-fusion proteins are more tightly packed in these structures and accordingly they exclude RFP-PTS1 (Fig. 3E and F).

It is a difficult task to distinguish GFP-HexA structures that move within a peroxisome from others that are attached to the membrane of motile peroxisomes. However, the series of images shown in Fig. 3A–D′ suggests an association of the donut-shaped GFP-HexA structures with the peroxisomal membrane. Thus, we found two localizations for GFP-HexA in the peroxisomes of the Δ*wsc*A mutant: (i) molecules which are dispersed in the luminal space, where they co-localize with RFP-PTS1 and (ii) molecules that are part of compact donut-shaped assemblies that may be somehow attached to the peroxisomal membrane.

### 2.3. Characterization of fusion proteins of WscA and GFP

We first analyzed the spatial distribution of a fusion of GFP to the C-terminus of WscA (WscA-GFP) in wild type hyphae relative to the peroxisomal marker RFP-PTS1, an approach that was successfully undertaken in *N. crassa* (Liu et al., 2008). As shown in Fig. 4A–D, WscA-GFP was found in large peroxisomes, but also in smaller spot-like structures that lacked RFP-PTS1. The latter were clearly anchored at septal pores and thereby resembled mature WBs (Fig. 4, arrows). However, most WscA-GFP was found in the membrane of large peroxisomes (Fig. 4E – G). The high resolution image shown in panel H indicates an uneven distribution of GFP-WscA in the peroxisomal membrane. After expression of WscA-GFP in the Δ*wsc*A mutant, HexA-containing structures were only detectable in 46% of the septa (Fig. 1A) indicating that the fusion protein is not able to fully replace WscA function. Surprisingly, expression of WscA-GFP in the control strain AfS35 reduced the percentage of septa with WB to 55% (Fig. 1A), indicating that this fusion protein even impairs the function of wild type WscA.

A C-terminal fusion of GFP interferes with the biological activity of WscA. We therefore tested whether an N-terminal fusion shows a different phenotype. After expression in *A. fumigatus*, GFP-WscA was only detectable in few, larger organelle-like structures (Fig. 5A). There were clearly fewer GFP-WscA aggregates than WBs in the wild type. GFP-WscA positive structures contained HexA, but HexA was also found in smaller spot-like structures that lacked

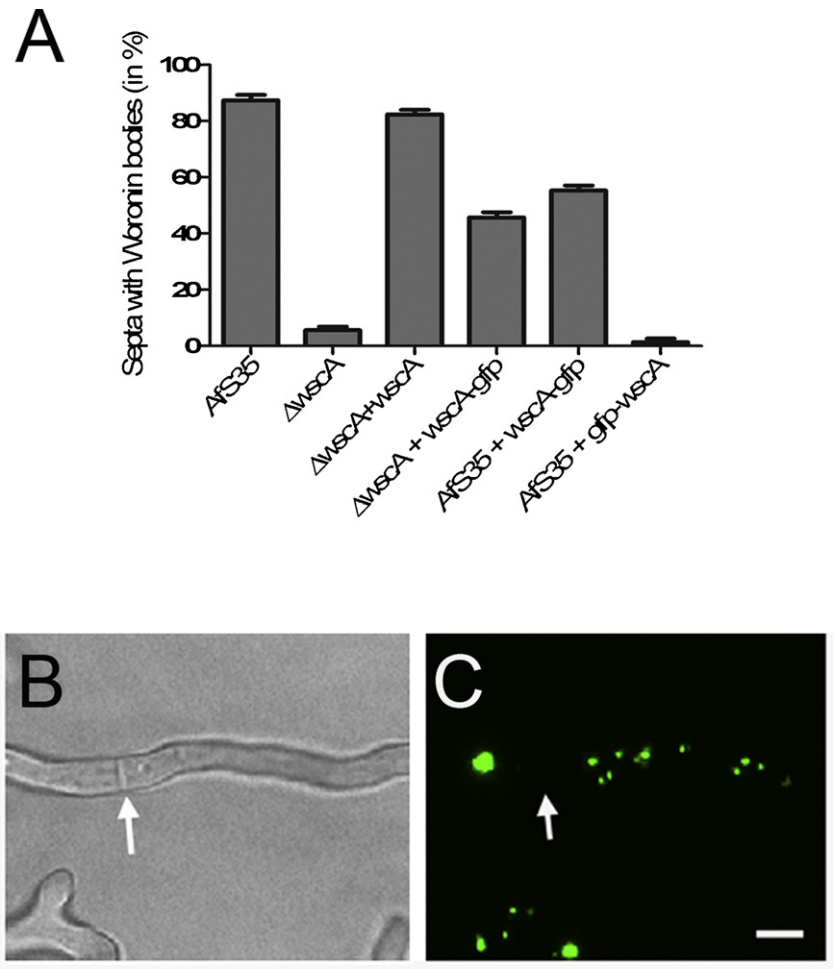


**Fig. 1.** The spatial distribution of HexA was analysed by immunofluorescence. The percentage of septa with HexA assemblies in their vicinity is given the Δ*wsc*A mutant, its parental strain AfS35 and derivative strains thereof expressing the indicated fusion proteins (A). Each value is representative for five data sets (with 50 septa per set). Standard deviations are indicated. A representative immunofluorescence micrograph and the corresponding bright field image are shown in C and B, respectively. The bar represents 4 μm.

GFP-WscA (Fig. 5A, arrows). Remarkably, hardly any of said HexA-positive structures, which in part resemble WBs in size, were found in the vicinity of septal pores (Fig. 1A). The overall weaker HexA signals for the GFP-WscA expressing strain observed in immunofluorescence correlated to a reduced amount of the 25 kDa form of HexA in whole protein extracts (Fig. 5E), whereas expression of WscA-GFP had no impact on the HexA protein level. Thus, in the wild type, GFP-WscA had a much stronger negative impact on the biogenesis and positioning of WBs than WscA-GFP.

### 2.4. *WscA is not required for the interaction between HexA and lah*

In general, the data presented so far are principally in line with the concept of WscA being required for the tethering of WBs to the septal pore. However, the Δ*wsc*A mutant lacks WBs and the localization of the remaining HexA aggregates provides no clues to the potential role of WscA in WB positioning. In *N. crassa*, WSC and LAH-1 interact and thereby link the organelle to the lateral cell wall. However, the two relevant domains are not conserved in most *Pezizomycotina*, which implies an alternative tethering mechanism. An interaction between HexA and Lah has been suggested by the distinct localization of a HexA-GFP fusion protein. In this fusion, the PTS1 motif of HexA is blocked by the GFP moiety thereby preventing an peroxisomal import. HexA-GFP is instead targeted to the septal pore in a Lah-dependent manner, implying that HexA may be directly involved in the binding of Lah to the Woronin body surface (Beck et al., 2013a). The Δ*wsc*A mutant allowed us to analyse a potential role of WscA in this interaction. In the Δ*wsc*A mutant, HexA-GFP is targeted to the septal pore as in the wild type (Fig. 6). This clearly demonstrates that WscA is not required for the interaction between HexA-GFP and Lah.

## 3. Discussion

The *A. fumigatus* protein WscA and *N. crassa* WSC are homologous and share a similar architecture. WscA resembles WSC also in its biological function: both proteins are targeted to the peroxisomal membrane, where they are essential for WB biogenesis. However, deletion mutants in the respective genes show also remarkable differences indicating that both proteins evolved according to their specific roles in WB partitioning and positioning.

An obvious phenotypical difference between both mutants is the striking enrichment of HEX protein assemblies in the apical compartment of the *N. crassa* mutant (Liu et al., 2008) that was not detectable in the Δ*wsc*A mutant. Instead, HexA is found in large peroxisomes in all hyphal compartments. Thus, the so far unknown mechanism that retains HEX assemblies to the apical compartment of the *N. crassa* mutant, does not exist in *A. fumigatus*.

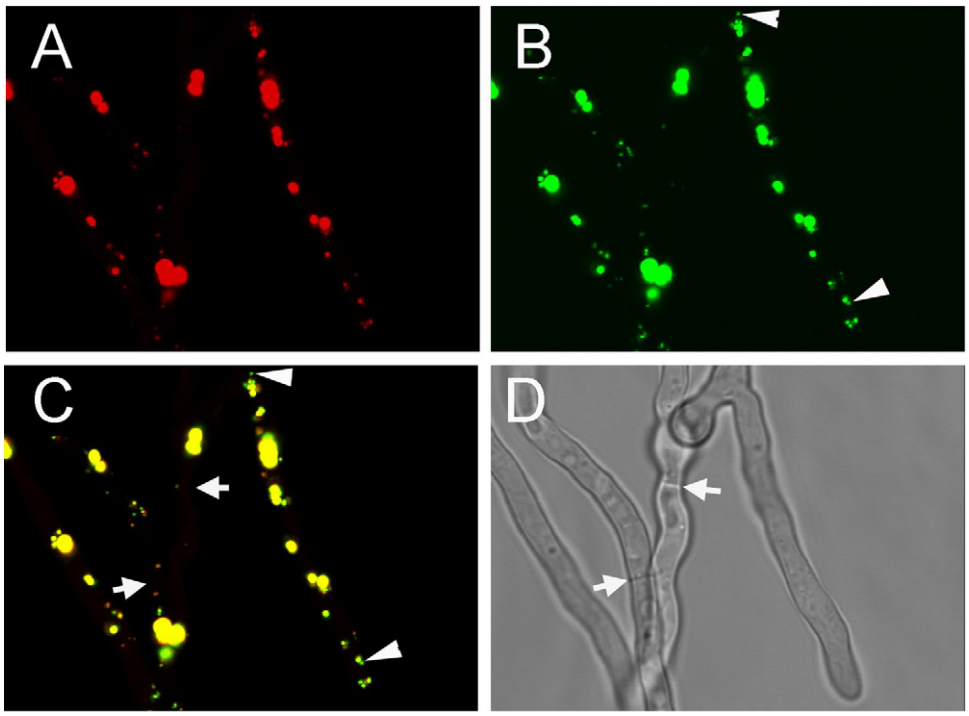


**Fig. 2.** Localisation of GFP-HexA and RFP-PTS1 in the Δ*wsc*A mutant. The spatial distribution of the peroxisomal marker RFP-PTS1 and GFP-HexA is shown in panel A and B, respectively. The corresponding overlay and bright field images are depicted in panel C and D, respectively. Septa are indicated by arrows, arrowheads point the small organelles harbouring GFP-HexA, but lacking RFP-PTS1. Panels A–C show maximum projects covering whole hyphae. Panel D represents a single optical plane.

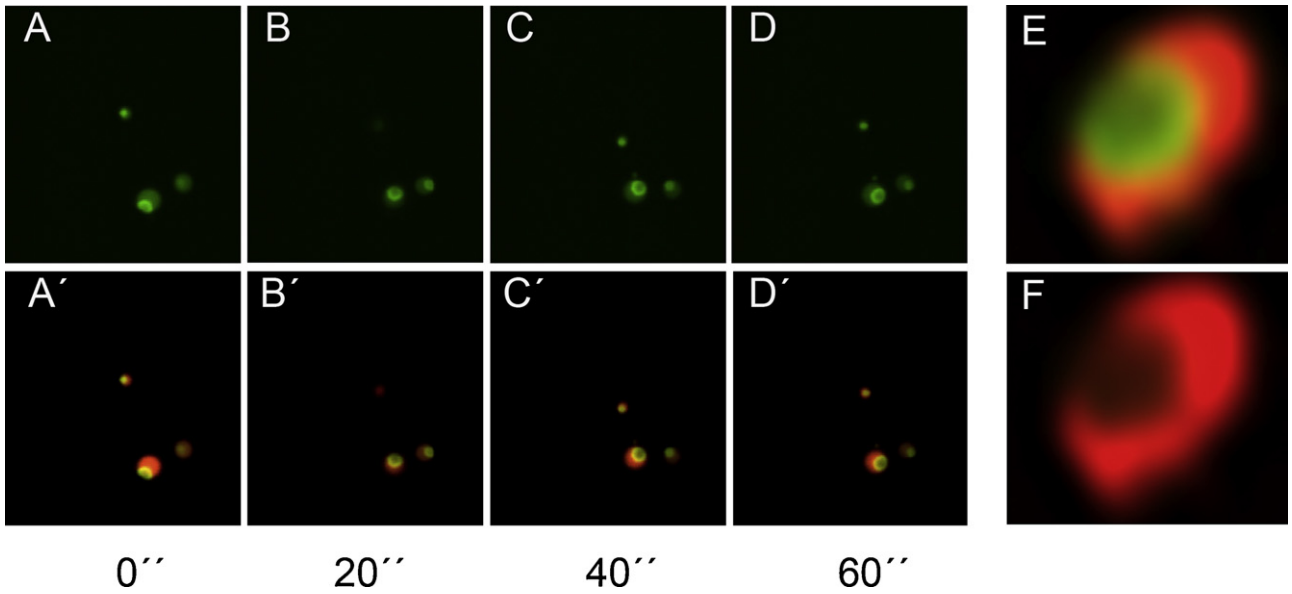


**Fig. 3.** Live cell imaging of GFP-HexA and RFP-PTS1 in the Δ*wsc*A mutant (A–D′). Large peroxisomes containing GFP-HexA and RFP-PTS1 were imaged every 20 s. Note the presence of donut-shaped structures that are enriched for GFP-HexA and the co-localization of GFP-HexA and RFP-PTS-1 in the remaining luminal space. High resolution images of a peroxisome containing GFP-HexA and RFP-PTS-1 are shown in E and F. Note the exclusion of RFP-PTS1 from the GFP-HexA assembly. All images represent single optical planes.

The *wsc*A deletion mutant does not form WBs anymore, but shows normal growth, colony morphology and conidiation, indicating that it is not significantly impaired under standard growth conditions. The mutant has a slightly increased sensitivity to the cell wall stressor Calcofluor white, but in the absence of stress, hyphal damage is not observed. This is remarkable, since increased cytosolic bleeding under normal growth conditions was exploited to identify the *wsc* gene in a screening of *N. crassa* mutants (Liu et al., 2008). One possible explanation for the robustness of the Δ*wsc*A mutant is that large, HexA-containing peroxisomes are found in all hyphal compartments. After wounding, these organelles may partially take over WB functions and close septal pores.

Concerning the localization of the Hex proteins, more subtle differences exist between the *wsc* and the *wsc*A deletion mutants. In the *Neurospora* mutant, GFP-HEX is exclusively found in hexagonal assemblies that move randomly in the lumen of large peroxisomes (Liu et al., 2008). In the Δ*wsc*A mutant, most GFP-HexA is also found in large peroxisomes, but its spatial distribution in

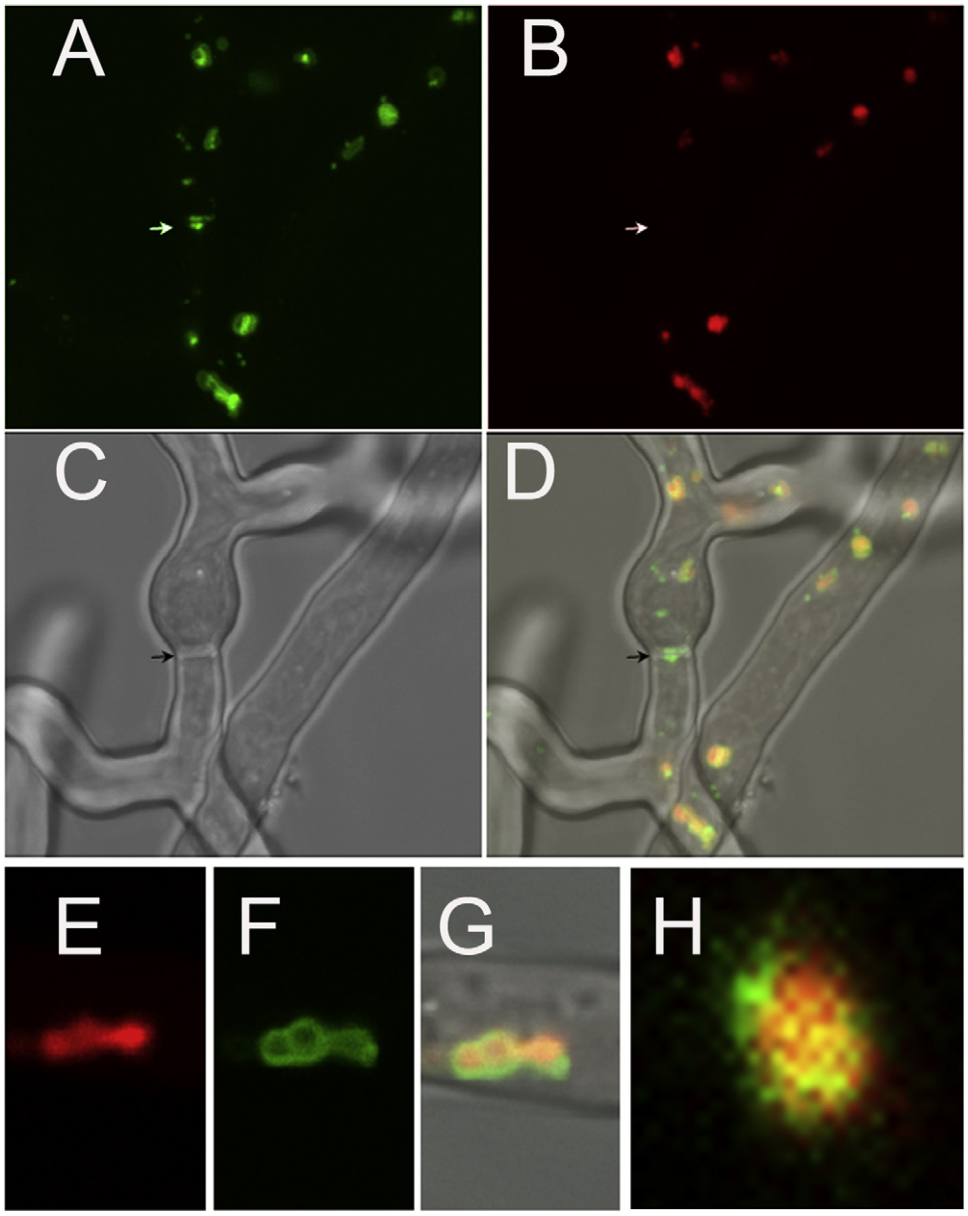


**Fig. 4.** Localisation of WscA-GFP. Panels A–D: after expression of WscA-GFP in the *A. fumigatus* strain AfS35, the fusion protein (green) was either detected in Woronin bodies at the septum (arrows) or in larger organelles also containing RFP-PTS1 (red). The images are a projection of a stack of confocal images representing the whole hyphae. Most WscA-GFP was found in these peroxisomes. Images in panels E–G demonstrate the localization of WscA-GFP in the peroxisomal membrane. The high resolution image of a single optical plane shown in panel H suggests an uneven distribution of WscA-GFP on the peroxisomal surface. (For interpretation of the references to color in this figure legend, the reader is referred to the web version of this article.)

the organelles differs. GFP-HexA co-localizes with the peroxisomal marker RFP-PTS1 in the luminal space, except for compact, donut-shaped GFP-HexA assemblies that exclude RFP-PTS1. Thus, a substantial portion of GFP-HexA seems to be dispersed in the peroxisomal lumen and consistently, these large peroxisomes have a variable shape. Within the donut-shaped structures, GFP-HexA molecules are apparently more tightly packed. The potential membrane association of these structures is puzzling, given that this strain lacks WscA, whose homolog in *N. crassa* was shown to mediate the interaction between the HEX proteins to the peroxisomal membrane (Liu et al., 2008). If the compact GFP-HexA structures are attached to the peroxisomal membrane, this is due to an alternative, WscA-independent mechanism.

In order to localize WscA, we have generated GFP fusion proteins. In *N. crassa*, expression of WSC-GFP leads to a strong enrichment of this fusion proteins in cortex-associated, mature WBs and in peroxisomal membranes at the sites of nascent WBs (Liu et al., 2008). This localization perfectly matches the assumed localization of native WSC and indicates that WSC-GFP is fully functional, which is remarkable, given that the C-terminus of WSC interacts with the tethering protein LAH-1 (Ng et al., 2009). In *A. fumigatus*, WscA-GFP is correctly targeted to the peroxisomal membrane, but only a certain percentage of these fusion proteins is found in WBs, both in the wild type and the *wsc*A mutant. This reflects an overall inefficient targeting of WscA-GFP to WBs. Moreover, WscA-GFP can only partially complement the *wsc*A mutant with respect to WB positioning. A fusion of GFP to the N-terminus of WscA had an even more remarkable impact, since GFP-WscA severely impairs WB biogenesis and completely abrogates WB positioning in the wild type, i.e. in the presence of native WscA.

WscA belongs to a family of peroxisomal proteins for which PMP22 is the eponymous member. These proteins harbour four

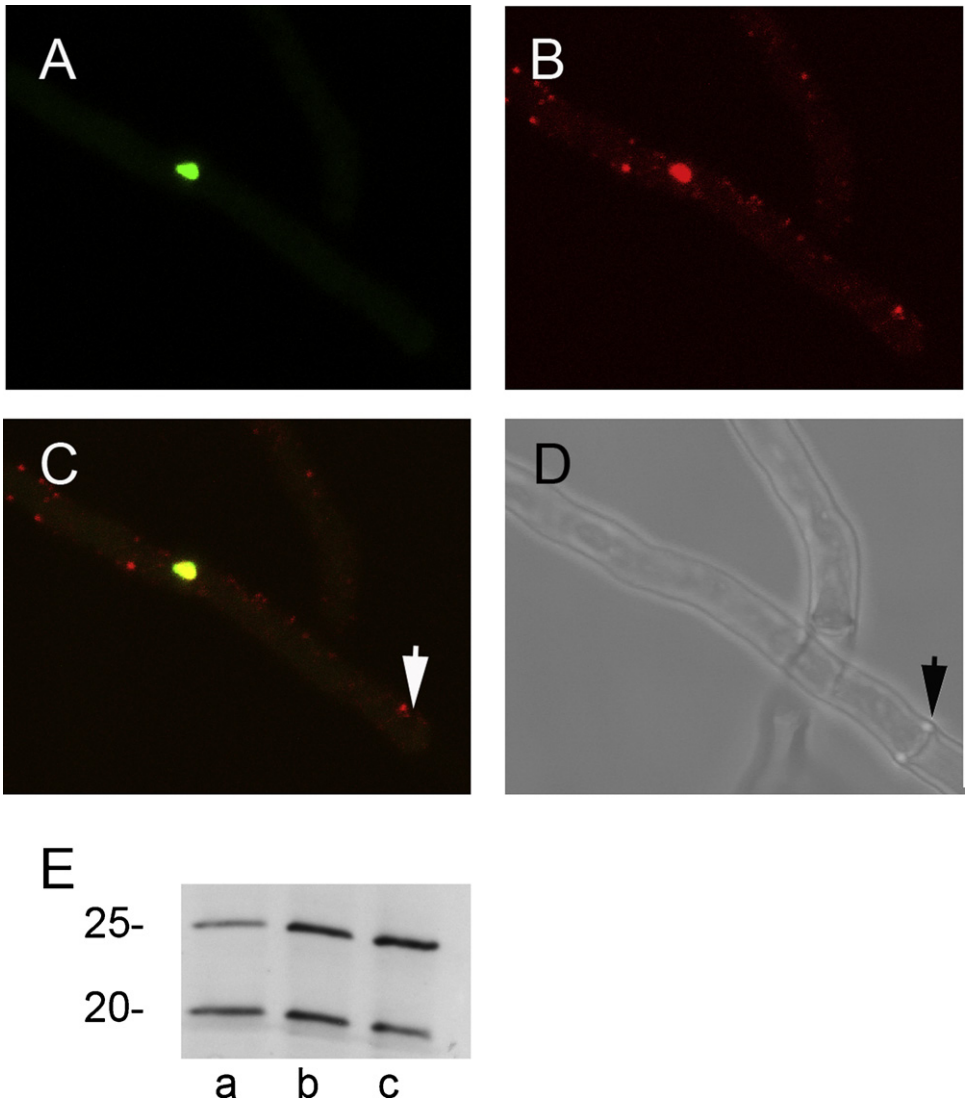


**Fig. 5.** Localisation of GFP-WscA in *A. fumigatus*. GFP-WscA expressed in the strain AfS35 is targeted to few spot-like structures that also contain HexA as demonstrated by immunofluorescence using the HexA-specific antibody Y191 (panels A and B, respectively). An overlay of green and red signals shows that HexA is also present in smaller structures that lacked GFP-WscA. Hardly any of these putative WBs was found in proximity to a septal pore. One septum is indicated by an arrow in panels C and D. Note that one WB is at the lateral wall and not associated with the central pore of the septum. Panels A– C represent stacks of optical planes, whereas panel D depicts only one optical plane. Panel E shows an immunoblot with the HexA-specific antibody Y157. Comparable amounts of whole cell extracts of the strain AfS35 + GFP-WscA (a), AfS35 + WscA-GFP (b) and the parental control AfS35 (c) have been analyzed. Selected molecular weight standards are indicated in kDa. (For interpretation of the references to color in this figure legend, the reader is referred to the web version of this article.)

membrane-spanning regions and at least some assemble into oligomers to form channels in the peroxisomal membrane (Brosius et al., 2002; Rokka et al., 2009; Antonenkov and Hiltunen, 2012). WSC also assembles into membrane-bound oligomers that interact with HEX and thereby initiate an essential step in WB biogenesis (Liu et al., 2008). Fusing GFP to WscA may interfere with the formation of functional oligomers by steric hindrance, which may consequently result in a less efficient WB positioning at the septum. The fusion of GFP to the N-terminus of WscA has a particularly severe phenotype. The bulky GFP domains in this fusion may even prevent formation of functional oligomers and thereby impair WB biogenesis. In immunoblot analysis, reduced amounts of the larger, 25 kDa form of HexA were detectable in whole cell extracts of the GFP-WscA expressing strain. A potential explanation is that WscA-GFP impedes the import of these HexA molecules into the peroxisomal lumen and those molecules that accumulate in the cytosol may then be degraded. However, in the Δ*wsc*A mutant, the import of HexA into the peroxisomal lumen seems to operate normally, which would speak against a role of WscA in the peroxisomal import of HexA. In conclusion, the severe, negative impact of GFP-WscA on the biogenesis and function of WBs in the *A. fumigatus* wild type is remarkable, but difficult to explain.

*Neurospora* differs from most other *Pezizomycotina* by the positions where WBs are anchored (cortical cell wall versus septal pore), which is a consequence of different positioning machineries. In *N. crassa* WSC interacts with LAH1 (Ng et al., 2009), but the relevant protein domains (the C-terminus of WSC and the N-terminus of LAH-1) are not conserved in *A. fumigatus,* indicating an alternative tethering mechanism. In *A. fumigatus*, the Lah receptor has not been unambiguously identified yet, but some evidence points to the N-terminal part of HexA, since HexA-GFP and certain truncated versions thereof are targeted to the septal pore in a Lah-dependent manner (Beck et al., 2013a). In the current study, we show that in the *wsc*A mutant, HexA-GFP is targeted to the septal pore as in the wild type, indicating that WscA it is not required for this process. However, in the wild type situation, WscA may nevertheless play an

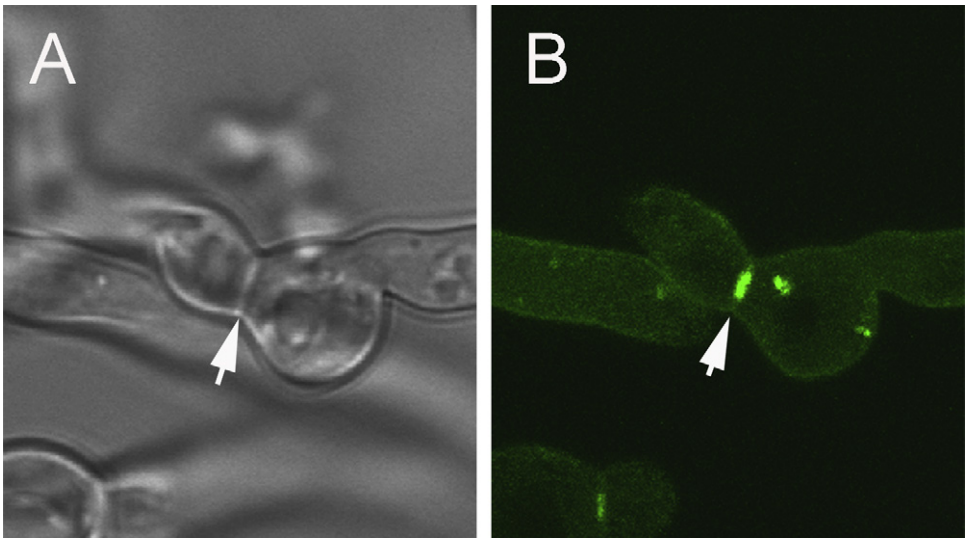


**Fig. 6.** Localisation of HexA-GFP in the Δ*wsc*A mutant. After expression of HexA-GFP in the Δ*wsc*A mutant, GFP-HexA is targeted to the vicinity of the septal pore. Note that in HexA-GFP the PTS1 targeting sequence is blocked by the GFP moiety.

**Table 1**
Strains used in this study.

| Strain | Parental strain | Source |
|---|---|---|
| AfS35 | D141 | Krappmann et al., 2006 |
| ΔhexA | AfS35 | Beck et al., 2013a |
| ΔwscA | AfS35 | This study |
| ΔwscA + wscA | AfS35 | This study |
| ΔwscA + wscA-gfp | AfS35 | This study |
| ΔwscA + gfp-HexA + rfp-PTS1 | AfS35 | This study |
| ΔwscA + hexA-gfp | AfS35 | This study |
| AfS35 + wscA-gfp | AfS35 | This study |
| AfS35 + gfp-wscA | AfS35 | This study |
| AfS35 + gfp-hexA + rfp-PTS1 | AfS35 | This study |
| **Reporter constructs** | | **Source** |
| rfp-PTS1 | | Beck and Ebel, 2013 |
| hexA-gfp | | Beck and Ebel, 2013 |
| gfp-hexA | | Beck et al., 2013a |
| wscA-gfp | | This study |
| gfp-wscA | | This study |

important role in the tethering of WBs. WscA oligomers may form a pore in the WB membrane to allow HexA molecules in the periphery of the core structure to extend their N-terminal domains into the cytoplasm, where they interact with the N-terminal domain of Lah.

In conclusion, we found that WscA and WSC have similar functions in WB biogenesis, but differ in other aspects, e.g. their role in WB positioning. The distinct properties of the Δ*wsc*A mutant provide further insights into the machinery that tethers WBs to the septal pores of *A. fumigatus*.

## 4. Material and methods

### 4.1. Strains and media

The *A. fumigatus* strain AfS35 is a derivative of strain D141 lacking the homologous end-joining component AkuA (Krappmann et al., 2006). A list of the strains used in this study is provided in Table 1. Aspergillus minimal medium (AMM) was prepared as described (Pontecorvo et al., 1953).

### 4.2. Sequence analysis and data base searches.

*A. fumigatus* sequences were obtained from the AspGD data base (http://www.aspgd.org/). Homology searches were performed using BlastP at Fungal Genomes Central—NCBI—NIH (http://www.ncbi.nlm.nih.gov/projects/genome/guide/fungi/) or Fungal Genomes Search at the Saccharomyces Genome Database (http://www.yeastgenome.org/blast-fungal). Transmembrane regions were identified using TMpred (http://www.ch.embnet.org/software/TMPRED_form.html) and protein localization predictions were performed using WoLF PSORT II (www.genscript.com./wolf-psort.html). Sequence alignments were generated using CLUSTAL OMEGA (http://www.ebi.ac.uk/Tools/msa/clustalo/).

### 4.3. Construction of the ΔwscA mutant

To delete the *wsc*A, flanking regions of approximately 1000 bp each were amplified using oligonucleotide combinations Wsc-up-FOR/Wsc-up-REV and Wsc-down-FOR/Wsc-down-REV. The resulting fragments were digested at primer derived SfiI sites and subsequently ligated to a 3.5 kb hygromycin resistance cassette flanked by compatible SfiI sites. The deletion cassette was then introduced into strain AfS35 using protoplast transformation (Punt and van den Hondel, 1992). For complementation, wscA was amplified using oligonucleotides Wsc-FOR and Wsc-STOP-REV and cloned into the PmeI site of pSK379. The mutant and the complemented strain were genetically verified by PCR using the primer combinations indicated in Suppl. Fig. 2. All genetic constructs that were later on expressed in *A. fumigatus* were amplified using Q5High Fidelity DNA Polymerase (New England Biolabs, Ipswich, MA, USA) and subsequently sequenced. The oligonucleotides used in this study are summarized in Table 2.

### 4.4. Construction of strains expressing fluorescent fusion proteins

The constructs used to express HexA-GFP, GFP-HexA and RFP-PTS1 have been described previously (Beck and Ebel, 2013; Beck et al., 2013a). To generate the WscA-GFP construct, the *wscA* sequence (without STOP codon) was amplified using oligonucleotides Wsc-FOR and Wsc-REV. The resulting fragment was cloned into the PmeI site of pSK379sGFP. For the GFP-WscA construct, the *wscA* gene was amplified using oligonucleotides

**Table 2**
Oligonucleotides used in this study.

| Designation | Sequence | Restriction site |
|---|---|---|
| Wsc-up-FOR | GTCCTGTTGTTATGCAGCATACAGGCA | |
| Wsc-up-REV | ATCGAT**GGCC**TGAGT**GGCC**GGTTGCTGGTGTTTATTT | SfiI |
| Wsc-down-FOR | ATCGAT**GGCC**ATCTA**GGCC**AGCCCCGCTAATATGCAG | SfiI |
| Wsc-down-REV | CCAGCTGAACCAGACCTCTTCCGCCGC | |
| Wsc-For | ATGTCGGTCAAGTTTCAGGAAGAGGCCACCAGGT | |
| Wsc-Rev | CGCCGGTAGTCGCCGCCCTTC | |
| Wsc + 1-FOR | CATGTCGGTCAAGTTTCAGGAAGAGGCCAC | |
| Wsc-STOP-REV | TTACCGGTAGTCGCCGCCCTTCTC | |
| seq-gpdA(p) | ACTCCATCCTTCCCATCCC | |
| hph-3-SmaI | T**CCCGGG**CTATTCCTTTGCCCTCGGACGAG | SmaI |

Wsc + 1-FOR and Wsc-STOP-REV and cloned into the EcoRV site of pSK379sGFP. Constructs were verified by sequencing.

### 4.5. Protein extraction and western blot

Hyphal proteins were extracted as described previously (Beck and Ebel, 2013). SDS-PAGE and immunoblot were performed according to standard procedures using the HexA-specific monoclonal antibody Y157 (Beck and Ebel, 2013) and alkaline phosphatase conjugated secondary antibodies.

### 4.6. Fluorescence imaging

Hyphae or germlings grown on glass cover slips in AMM at 30 °C were fixed with 3.7% formaldehyde/PBS and washed twice with PBS. For cell wall digestion, samples were incubated in 300 μl PBS containing 10 mg bovine serum albumin and 6 mg lysing enzymes from *Trichoderma harzianum* (Sigma) for 1 h at 37 °C. Treated cells were then permeabilized with 0.2% Triton X-100 in PBS for 1 min and subsequently blocked with 2% goat serum/PBS for one hour. After three brief washing steps with PBS, samples were incubated with the HexA-specific antibody Y191 in a humid chamber for 30 min and washed another three times with PBS. Bound antibodies were stained using Cy3-labelled anti-mouse immunoglobulin (Dianova, Hamburg, Germany). After a final washing step, samples were mounted with Vecta Shield (Vector Laboratories, Burlingame, California, USA). Images shown in Fig. 3E and F and Fig. 4H were taken with a Zeiss LSM880 with Airyscan (Zeiss, Oberkochen, Germany), all other images were taken using a Leica SP5 microscope (Leica Microsystems, Wetzlar, Germany).

### 4.7. Quantitative analysis of WB positioning

To determine the percentage of septa with associated WBs we stained the respective hyphae in immunofluorescence with Y191. Stacks of confocal images were then acquired and analysed that covered hyphae in their whole depth (distance of 0.5 μm between individual optical planes). Septa were counted as positive, if HexA assemblies were found in close proximity to the pore. The percentages of septa with associated WBs were determined for 5 sets of 50 septa each.

### 4.8. Live cell imaging

To analyse fluorescent fusion proteins, conidia of the respective strains were inoculated in 8-well ibidi-chambers or 60 μ-dishes (ibidi GmbH, Martinsried, Germany) containing AMM. Germ tubes were generated by overnight incubation at 30° C. Fungal cells were then grown to the desired length and the samples were analysed using a Leica SP-5 microscope equipped with an environmental chamber adjusted to 37 °C (Leica Microsystems).

## Acknowledgements

We thank Jan Erik Heil (ZEISS Microscopy Labs, Munich) for his help with confocal microscopy and Kirsten Niebuhr for critical reading of the manuscript. This project was supported by a grant from the FoeFoLe program of the Medical Faculty of the Ludwig-Maximilians-University.

## Appendix A. Supplementary data

Supplementary data associated with this article can be found, in the online version, at http://dx.doi.org/10.1016/j.ijmm.2016.03.008.

## References

Antonenkov, V.D., Hiltunen, J.K., 2012. Transfer of metabolites across the peroxisomal membrane. Biochim. Biophys. Acta 1822, 1374–1386.
Beck, J., Ebel, F., 2013. Characterization of the major Woronin body protein HexA of the human pathogenic mold *Aspergillus fumigatus*. Int. J. Med. Microbiol. 303, 90–97.
Beck, J., Wagener, J., Ebel, F., 2013. The septal cell wall of filamentous fungi. In: Manuel Mora-Montes, H. (Ed.), The Fungal Cell Wall. Nova Publishers, pp. 129–142.
Beck, J., Echtenacher, B., Ebel, F., 2013a. Woronin bodies, their impact on stress resistance and virulence of the pathogenic mould *Aspergillus fumigatus* and their anchoring at the septal pore of filamentous Ascomycota. Mol. Microbiol. 89, 857–871.
Bleichrodt, R.J., van Veluw, G.J., Recter, B., Maruyama, J., Kitamoto, K., Wösten, H.A., 2012. Hyphal heterogeneity in *Aspergillus oryzae* is the result of dynamic closure of septa by Woronin bodies. Mol. Microbiol. 86, 1334–1344.
Brosius, U., Dehmel, T., Gärtner, J., 2002. Two different targeting signals direct human peroxisomal membrane protein 22 to peroxisomes. J. Biol. Chem. 277, 774–784.
Collinge, A.J., Markham, P., 1985. Woronin bodies rapidly plug septal pores of severed *Penicillium chrysogenum* hyphae. Exp. Mycol. 9, 80–95.
Dichtl, K., Samantaray, S., Aimanianda, V., Zhu, Z., Prévost, M.C., Latgé, J.P., Ebel, F., Wagener, J., 2015. *Aspergillus fumigatus* devoid of cell wall $\beta$-1,3-glucan is viable, massively sheds galactomannan and is killed by septum formation inhibitors. Mol. Microbiol. 95, 458–471.
Jedd, G., Chua, N.H., 2000. A new self-assembled peroxisomal vesicle required for efficient resealing of the plasma membrane. Nat. Cell Biol. 2, 226–231.
Krappmann, S., Sasse, C., Braus, G.H., 2006. Gene targeting in *Aspergillus fumigatus* by homologous recombination is facilitated in a nonhomologous end-joining-deficient genetic background. Eukaryot. Cell 5, 212–215.
Liu, F., Ng, S.K., Lu, Y., Low, W., Lai, J., Jedd, G., 2008. Making two organelles from one: Woronin body biogenesis by peroxisomal protein sorting. J. Cell Biol. 180, 325–339.
Maruyama, J., Kitamoto, K., 2013. Expanding functional repertoires of fungal peroxisomes: contribution to growth and survival processes. Front. Physiol. 4, 177.
McCormick, A., Loeffler, J., Ebel, F., 2010. *Aspergillus fumigatus*: contours of an opportunistic human pathogen. Cell. Microbiol. 12, 1535–1543.
Momany, M., Richardson, E.A., Van Sickle, C., Jedd, G., 2002. Mapping Woronin body position in *Aspergillus nidulans*. Mycologia 94, 260–266.
Ng, S.K., Liu, F., Lai, J., Low, W., Jedd, G., 2009. A tether for Woronin body inheritance is associated with evolutionary variation in organelle positioning. PLoS Genet. 5, e1000521.
Pontecorvo, G., Roper, J.A., Hemmons, L.M., MacDonald, K.D., Bufton, A.W., 1953. The genetics of *Aspergillus nidulans*. Adv. Genet. 5, 141–238.
Punt, P.J., van den Hondel, V.A., 1992. Transformation of filamentous fungi based on hygromycin B and phleomycin resistance markers. Methods Enzymol. 216, 447–457.

Rokka, A., Antonenkov, V.D., Soininen, R., Immonen, H.L., Pirilä, P.L., Bergmann, U., Sormunen, R.T., Weckström, M., Benz, R., Hiltunen, J.K., 2009. Pxmp2 is a channel-forming protein in mammalian peroxisomal membrane. PLoS One 4, e5090.

Tekaia, F., Latgé, J.P., 2005. *Aspergillus fumigatus*: saprophyte or pathogen? Curr. Opin. Microbiol. 8, 385–392.

Tell, L.A., 2005. Aspergillosis in mammals and birds: impact on veterinary medicine. Med. Mycol. 43, S71–S73.

Tenney, K., Hunt, I., Sweigard, J., Pounder, J.I., McClain, C., Bowman, E.J., Bowman, B.J., 2000. Hex-1, a gene unique to filamentous fungi, encodes the major protein of the Woronin body and functions as a plug for septal pores. Fungal Genet. Biol. 31, 205–217.

Woronin, M., 1864. Entwicklungsgeschichte des *Ascobolus pucherrimus* Cr. und einiger Pezizen. Abh. Senkenb. Naturforsch. 5, 355–444.

**4.2** Leonhardt, Y., Kakoschke, SC., Wagener, J. and Ebel, F. Lah is a transmembrane protein and requires Spa10 for stable positioning of Woronin bodies at the septal pore of *Aspergillus fumigatus*. Sci Rep. 2017;7:44179.

Seite 29 - 40

SCIENTIFIC REPORTS

OPEN

Received: 07 October 2016
Accepted: 06 February 2017
Published: 10 March 2017

# Lah is a transmembrane protein and requires Spa10 for stable positioning of Woronin bodies at the septal pore of *Aspergillus fumigatus*

Yannik Leonhardt[1,*], Sara Carina Kakoschke[1,*], Johannes Wagener[1] & Frank Ebel[1,2]

**Woronin bodies are specialized, fungal-specific organelles that enable an immediate closure of septal pores after injury to protect hyphae from excessive cytoplasmic bleeding. In most Ascomycetes, Woronin bodies are tethered at the septal pore by so-called Lah proteins. Using the pathogenic mold *Aspergillus fumigatus* as a model organism, we show that the C-terminal 288 amino acids of Lah ($LahC_{288}$) bind to the rim of the septal pore. $LahC_{288}$ essentially consists of a membrane spanning region and a putative extracellular domain, which are both required for the targeting to the septum. In an *A. fumigatus rho4* deletion mutant that has a severe defect in septum formation, $LahC_{288}$ is recruited to spot-like structures in or at the lateral membrane. This suggests that LahC is recruited before Rho4 starts to govern the septation process. Accordingly, we found that in wild type hyphae Lah is bound before a cross-wall emerges and thus enables a tethering of Woronin bodies at the site of the newly formed septum. Finally, we identified Spa10, a member of a recently described family of septal pore-associated proteins, as a first protein that directly or indirectly interacts with LahC to allow a stable positioning of Woronin bodies at the mature septum.**

Eukaryotic cells have a complex composition comprising different organelles and many other specialized substructures. To function properly these parts of the cellular machinery have to be arranged in a certain spatial pattern. The precise positioning of organelles therefore represents an important element of the cellular architecture. A fascinating example of such a positioning is the anchoring of Woronin bodies to the cell envelope of filamentous fungi. Two distinct spatial patterns have evolved: In the *Neurospora*/*Sordaria* clade, Woronin bodies are tethered to the lateral cell wall[1] whereas in most other Ascomycetes they are positioned directly at the septal pore[2] Woronin bodies protect hyphae from extensive cytoplasmic bleeding after damage. They have been shown to be important for the stress resistance and virulence of the plant pathogen *Magnaporthe grisea*[3] the nematophagous fungus *Arthrobotrys oligospora*[4] and the human pathogenic mold *A. fumigatus*[5]. In the latter, a lack of Woronin bodies furthermore results in an enhanced sensitivity for the cell wall-damaging antimycotic agent caspofungin[6].

Woronin bodies are fungal-specific organelles that derive from specialized peroxisomes[7] and contain two characteristic components. The so-called Hex protein assembles into a paracrystalline structure that fills the matrix of the Woronin body[8]. The other characteristic constituent is a membrane protein, designated WSC in *N. crassa* and WscA in *A. fumigatus*. Both proteins have been shown to be essential for the biogenesis of Woronin bodies, but they apparently differ with respect to their roles in the anchoring of Woronin bodies. WSC was shown to interact with the N-terminus of the leashin protein LAH-1[1] whereas such a direct involvement in the tethering process is unlikely for WscA[9].

The lateral binding pattern of Woronin bodies found in *Neurospora* is characteristic for a small group of fungi. It most likely developed from an ancestral pattern found in most other Ascomycetes to meet the specific

[1]Max-von-Pettenkofer-Institute, Ludwig-Maximilians-University, Munich, 80336, Germany. [2]Institute for Infectious Diseases and Zoonoses, Ludwig-Maximilians-University, Munich, 80539, Germany. *These authors contributed equally to this work. Correspondence and requests for materials should be addressed to F.E. (email: frank.ebel@lmu.de)

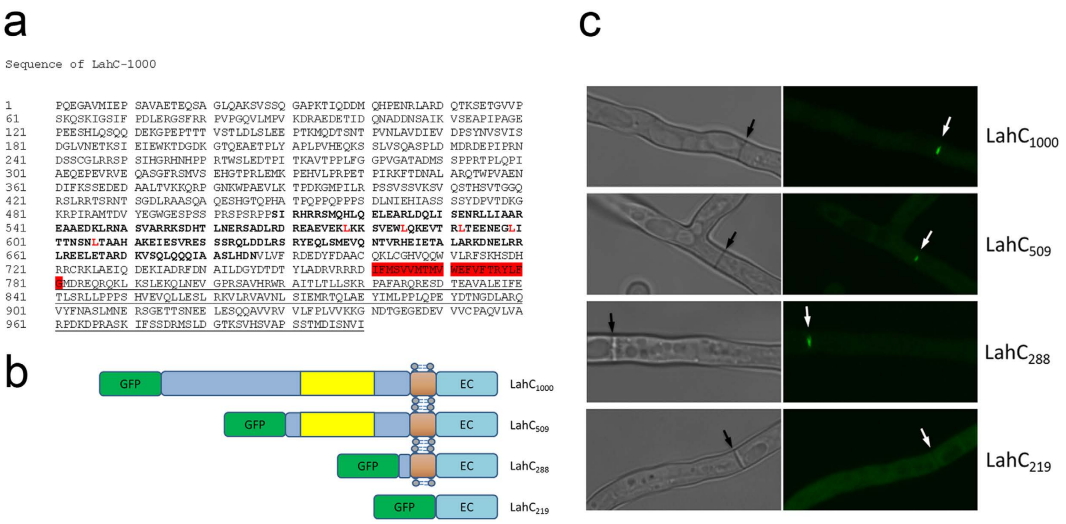


**Figure 1. Identification of the minimal LahC domain** . Panel (a) Sequence analysis of the C-terminal 1000 aa of Lah. The putative coiled-coil region is indicated in bold. The leucine residues of a putative leucine zipper are indicated in red. The predicted transmembrane region is highlighted in red. A region that is also conserved in *N. crassa* LAH-2, is underlined. Panel (b and c) GFP-LahC$_{1000}$ and several derivatives thereof containing truncated versions of LahC were generated. These constructs are schematically depicted in panel (b). The putative coiled-coil (yellow), transmembrane (brown) and extracellular domains (EC) are indicated. Panel (c) shows the localization of the different fusion proteins in *A. fumigatus* hyphae. Each image represents a projection of a stack of confocal images covering hypha in their whole depth. Arrows indicate the positions of septa.

requirements of fungi that grow unusually fast[10]. It is assumed that due to the characteristic cytoplasmic streaming towards the apical tips of *Neurospora*, septum-associated Woronin bodies would immediately block the septal pores. In most other Ascomycetes, Woronin bodies are positioned in close proximity to the septal pore and if activated can immediately close this connection to neighboring cells[2]. For this group of fungi, *Aspergillus* Lah is the prototypic leashin protein[5,11].

In eukaryotic cells, the positioning of organelles is often mediated by interactions with the cytoskeleton, which provides a physical frame work that spans the whole cell[12,13]. The positioning of Woronin bodies seems to be independent of cytoskeletal elements and instead relies on giant tethering proteins of approximately 500.000 Da. These proteins have been designated leashins to emphasize their common function that, however, is not always based on sequence homology. The leashin LAH-1 found in the *Neurospora/Sordaria* clade shows no homology to the Lah proteins of most other Ascomycetes[1,5] but both types of leashins link Woronin bodies either to the hyphal envelope or the septal pore. Thus, two distinct tethering proteins determine the two positioning patterns of Woronin bodies found in filamentous fungi.

We have recently shown that the N-terminal domain of the leashin Lah binds to the surface of Woronin bodies, whereas its C-terminal part is targeted to the rim of the septal pore[5]. The LahC domain that was initially described comprised 1000 amino acids (aa), which corresponds to a molecular weight of more than 110 kDa. In this study, we have narrowed down the LahC targeting domain to 288 aa. Moreover, we provide evidence that this domain harbors a membrane-spanning region that is essential for its function. Finally, we have identified Spa10 as the first septum-associated protein that is required for a stable anchoring of Woronin bodies at the septal pore.

## Results

**Sequence analysis of the C-terminal 1000 amino acids of Lah.** We have recently shown that the C-terminal 1000 aa of Lah are sufficient to target GFP to the central part of the septal cell wall[5]. In this study, we have further analysed the corresponding amino acid sequence (Fig. 1a). The SMART program predicts a coiled-coil domain comprising residues 509–686 including several leucine residues that may form a leucine zipper (as predicted by the 2ZIP–Server). A putative inside-to-outside transmembrane region was predicted for residues 761–781 by TMpred and PHOBIUS. Remarkably, we found that the transmembrane region is also conserved in *N. crassa* LAH-2 as well as in the Lah proteins of *A. nidulans* (FGSC A4), *A. oryzae* (RIB40), *A. terreus* (NIH2624) and *A. flavus* (NRRL 3357) (data not shown).

**A domain consisting of 288 amino acid targets Lah to the septal pore.** Starting from GFP-LahC$_{1000}$ we constructed a series of fusion proteins comprising smaller parts of the C-terminus of Lah (Fig. 1b). Fusions containing the C-terminal 509 (GFP-LahC$_{509}$) or 288 aa (GFP-LahC$_{288}$) showed the same targeting to the septum as GFP-LahC$_{1000}$ (Fig. 1c). LahC$_{288}$ lacks the putative coiled-coil domain, but comprises the predicted transmembrane region (Fig. 1b). GFP-LahC$_{219}$, which lacks this putative membrane-spanning segment, was not recruited to the septum, but evenly spread in the cytosol instead (Fig. 1b and c). This demonstrates that the putative transmembrane sequence is required for the correct targeting of LahC.

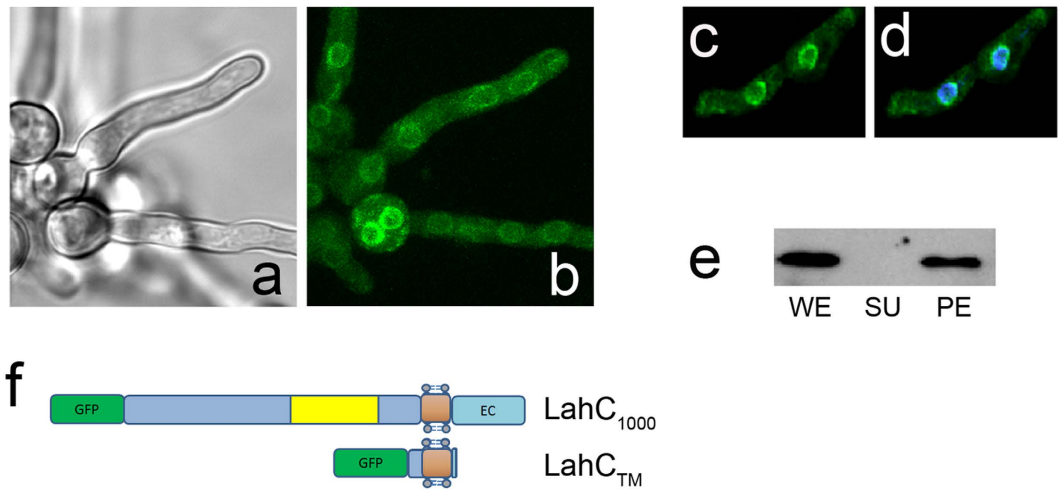


**Figure 2. GFP-LahC$_{TM}$ is a membrane protein and localizes to perinuclear organelle-like structures.** GFP-LahC$_{1000}$ and the GFP-LahC$_{TM}$ construct are schematically depicted in panel (f). The putative coiled-coil (yellow), transmembrane (brown) and extracellular domains (EC) are indicated. GFP-LahC$_{TM,}$ localizes in circular structures in the cytoplasm of *A. fumigatus* (panel b). Panel (a) shows a corresponding brightfield image. Panel (c) shows GFP-LahC$_{TM}$ fluorescence and panel (d) the corresponding overlay of GFP-LahC$_{TM}$ and DAPI fluorescence. Panel (e) shows an anti-GFP immunoblot of whole cell extract (WE), supernatant and pellet fraction obtained after ultracentrifugation (SU and PE, respectively).

In the next step, we generated another truncated derivative of GFP-LahC$_{288}$ lacking the putative extracellular domain. This fusion protein, designated GFP-LahC$_{TM}$, comprises the membrane spanning region and short stretches of flanking residues. As shown in Fig. 2b, it is not recruited to the septum, but enriched in circular, organelle-like structures in the cytoplasm. A parallel DAPI staining revealed a perinuclear pattern for this GFP fusion protein (Fig. 2c and d). These microscopic images already suggested that GFP-LahC$_{TM}$ is a membrane protein. To verify this, lysates of *A. fumigatus* expressing GFP-LahC$_{TM}$ were fractionated by ultracentrifugation and subsequently analysed by immunoblot. A GFP-fusion protein of the expected size was detectable in the whole cell lysate and in the pellet fraction, but not in the supernatant (Fig. 2e), which supports the notion that LahC$_{TM}$ is a membrane protein. To provide further evidence, we introduced two point mutations resulting in two amino acid substitutions ($V_{5303}\rightarrow E_{5303}$ and $V_{5304}\rightarrow E_{5304}$) that eliminated the predicted transmembrane sequence (Supplementary Fig. S1). The corresponding fusion protein, designated GFP-LahC$_{288}$*, is not targeted to the septal pore (Supplementary Fig. S1) demonstrating that the membrane-spanning segment is essentially required for a correct localization of LahC.

**LahC and Woronin bodies are recruited at an early time point during septation.** The Lah protein tethers Woronin bodies to the rim of the septal pore, but it was unknown whether LahC is recruited at an early or late stage of the septation process. In order to address this question, we analyzed hyphae by live cell microscopy. Figure 3 shows a hyphal segment with a newly formed septum. The images clearly show the formation and constriction of a GFP-LahC ring during septum formation. Strikingly, LahC is recruited even before a cross wall is visible (after 5 and 7.5 min). In a strain expressing GFP-LahC$_{288}$ and LifeAct-RFP, LahC appeared at the site of septation approximately at same time as the contractile actin ring (Supplementary Fig. S2). The early recruitment of LahC suggested that Woronin bodies may already been tethered at the sites of emerging septa. To address this point we generated an *A. fumigatus* wild type strain in which Woronin bodies are visualized by expression of LahN-GFP. As shown in Fig. 4, Woronin bodies indeed gather in the plane of the forming septum, before they are finally arranged in the characteristic cluster proximal to the septal pore. We also analysed the septation process in an *A. fumigatus* strain co-expressing LahN-GFP and LifeAct-RFP. A set of images is shown in the Supplementary Fig. 3. As soon as the newly formed septum became visible by bright-field microscopy, Woronin bodies appeared to be tethered at the emerging cross wall, whereas the formation of the contractile actin ring was evident 3 min earlier (Supplementary Fig. S3).

We have recently shown that an *A. fumigatus* Δ*rho*4 mutant has a severe defect in septum formation[14] Expression of GFP-LahC$_{288}$ in this mutant led to a striking localization pattern. GFP-LahC$_{288}$ was strongly enriched in spot-like structures (Fig. 5a) and cross-sections by confocal xz analysis showed that these structures localize in or at the lateral membrane (Fig. 5b). Live cell imaging revealed that these structures are stable and show a limited motility in the plane of the cytoplasmic membrane (Video 1). Live cell microscopy of a Δ*rho*4 mutant strain expressing GFP-HexA revealed that some GFP-tagged Woronin bodies were clearly associated with the lateral wall for longer times (Supplementary Fig. S4), a pattern that was never observed in the wild type (data not shown). In conclusion, our data suggest that in the absence of Rho4 certain protein complexes assemble in or at the cytoplasmic membrane that recruit GFP-LahC$_{288}$ and can thereby tether Woronin bodies.

**Analysis of the role of Spa10 during septum formation.** The data described so far suggest that the LahC receptor is a membrane protein with an extracellular domain that interacts with the extracellular domain

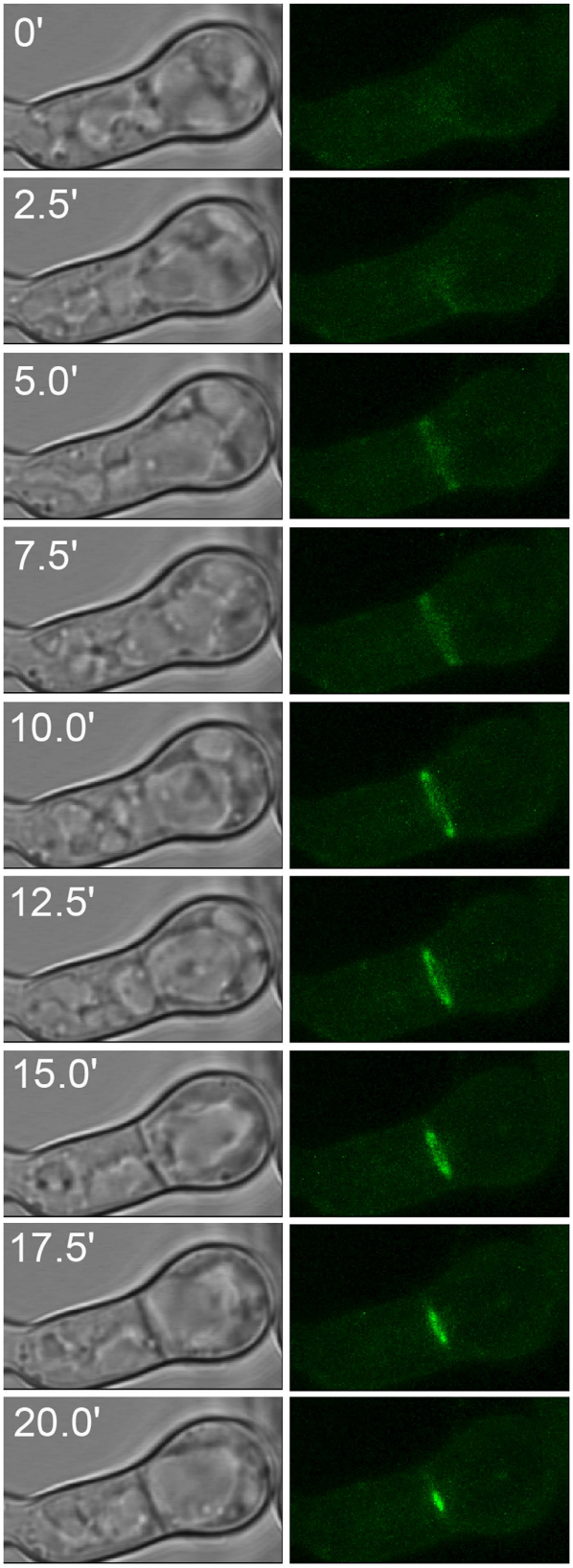


**Figure 3. Recruitment of LahC during septum formation.** Live cell imaging of an *A. fumigatus* strain expressing GFP-$LahC_{288}$. Images are projections of stacks of confocal images that were taken in intervals of 2.5 min.

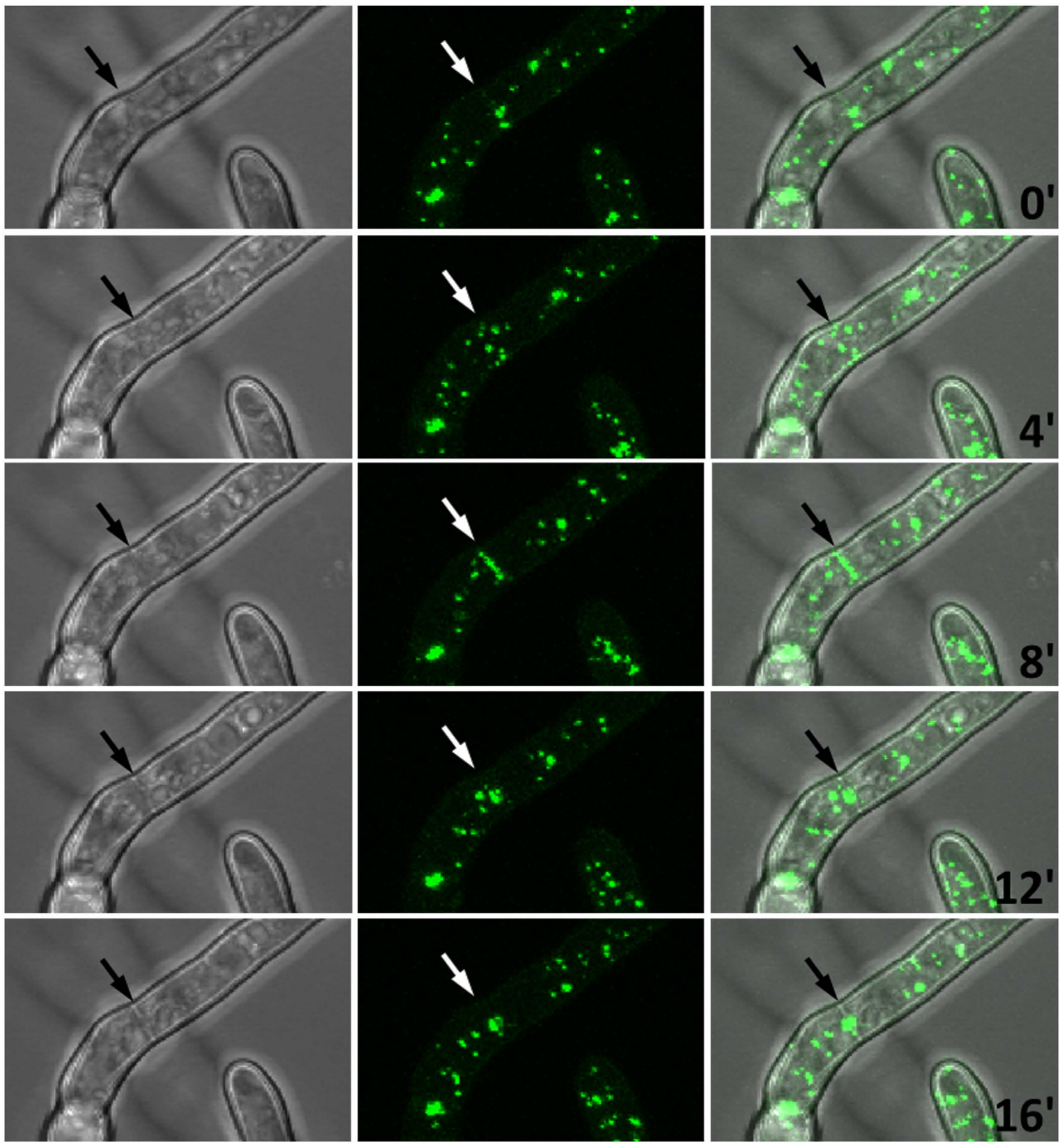


**Figure 4. Recruitment of Woronin bodies during septum formation.** Panels show *A. fumigatus* hyphae expressing LahN-GFP to visualize Woronin bodies. The micrographs are projections of stacks of confocal images that were taken every 4 min. Arrows indicate the position of an emerging septum.

of LahC. The putative LahC receptor is recruited early to the site of septation and shows a stable localization at the rim of the mature septal pore. Literature searches revealed a candidate for this receptor with a promising localization pattern, namely Spa10, which has briefly been characterized in *A. nidulans*[15]. Its *A. fumigatus* counterpart, encoded by Afu4g13320, is predicted to possess a membrane-spanning region with a high probability for an N-terminus-out configuration. We therefore constructed a Spa10-RFP fusion protein and expressed it in *A. fumigatus*. This fusion protein indeed localized to the septal cross-wall, but unlike LahC, this localization appeared to be less focussed around the septal pore (Supplementary Fig. S5). During septum formation in the wild type, Spa10-RFP appeared, when a septal cross wall was already visible by light microscopy (Supplementary Fig. S6). In the Δ*rho*4 mutant, Spa10-RFP was not recruited to discrete spot-like structures like GFP-LahC$_{288}$, but localized along the lateral membrane instead, a pattern that was particular prominent in conidial bodies (Supplementary Fig. S5). A closer inspection of wild type hyphae revealed a similar, but less prominent localization at the lateral cell wall (data not shown). The clearly distinct localisation patterns of Spa10-RFP and GFP-LahC in the Δ*rho*4 mutant argued against a direct interaction of these proteins. However, to investigate the role of Spa10 in the septation process in more detail, we generated an *A. fumigatus spa*10 deletion mutant. The generation and verification of this deletion is schematically depicted in Supplementary Fig. S7. The mutant showed no obvious defect in growth compared to wild type, both at 37 °C or 50 °C. In the presence of the cell wall stressor Calcofluor white the mutant grew like wild type and showed only a slight delay in conidiation (Supplementary Fig. S7). Analysis of septum formation by Calcofluor white staining revealed also no obvious defects for the mutant (data not shown).

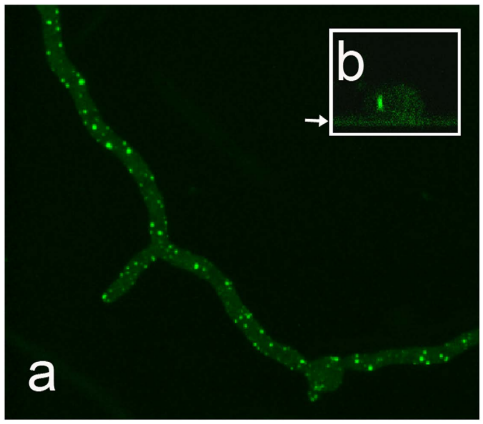


**Figure 5. Localization of GFP-LahC$_{288}$ in the Δ*rho*4 mutant.** Panel (a) shows the localization of GFP-LahC$_{288}$ in distinct spots. Panel (b) shows xz-cross sections of a hypha demonstrating that the GFP-LahC$_{288}$-positive spots localize at the lateral membrane. The position of the cover slip is indicated by an arrow.

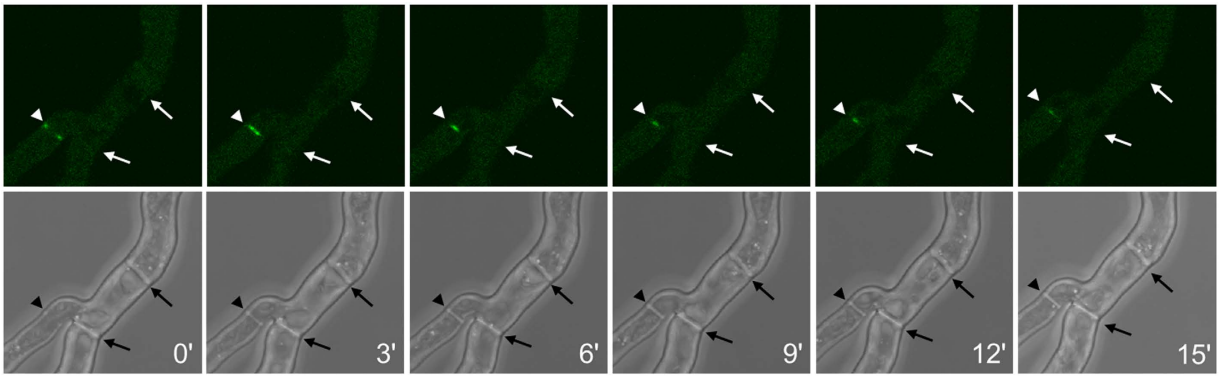


**Figure 6. Live cell imaging of GFP-LahC$_{288}$ in the Δ*spa*10 mutant.** Images represent projections of stacks of confocal images and were taken at 3 min intervals. Arrows indicate the positions of septa. The arrowheads indicate the position of a newly formed septum.

A striking phenotype of the Δ*spa*10 mutant became apparent after expression of GFP-LahC$_{288}$. Initially, we found no distinct localization of GFP-LahC$_{288}$ in this mutant, but a closer inspection revealed a striking recruitment of GFP-LahC$_{288}$ to the sites of newly formed septa (Fig. 6). As in wild type hyphae, GFP-LahC is recruited early, when a cross wall was hardly visible, and during the centripetal growth of the septal wall its localization became more and more focused to the center of the septation plane. Unlike wild type, the GFP-LahC-positive structures at the mature septum of the mutant lost their fluorescence over time. After 15 min these structures were hardly detectable and at later time points many of them disappeared completely (Fig. 6 and data not shown).

We hypothesized that the dramatically reduced amounts of LahC found at the mature septa of the Δ*spa*10 mutant should have consequences for the positioning of Woronin bodies. To prove this, we expressed GFP-HexA in this mutant. In the resulting strain, only very few Woronin bodies were found in proximity to a septum and live cell microscopy revealed that these associations were only accidental or transient (Fig. 7a). Expression of Spa10 or Spa10-RFP in the mutant restored the wild type phenotype with Woronin bodies anchored at either side of the septum (Fig. 8 and data not shown). Spa10-RFP was enriched in the vicinity of the septal pore, but in contrast to GFP-LahC$_{288}$, also found at other parts of the septal cross wall (Fig. 8).

Using live cell imaging, we also determined the average time a Woronin body remained at the septal pore (Fig. 7b). These experiments were run for up to 60 min. All Woronin bodies in the wild type and the complemented Δ*spa*10 mutant (*spa*10 or *spa*10-*rfp*) remained at the septum for the whole time period, only the Δ*spa*10 mutant showed a striking defect with an average time of 9.0 min. Another feature of this mutant that distinguishes it from the wild type is the tendency of Woronin bodies to form clusters (Fig. 7a), a pattern resembling that found in a mutant expressing a truncated Lah protein, which lacks its C-terminal domain[5]. In conclusion, our data demonstrate that in the absence of Spa10, LahC is unable to reside at the mature septal pore and consequently Woronin bodies cannot or only transiently associate with the septum.

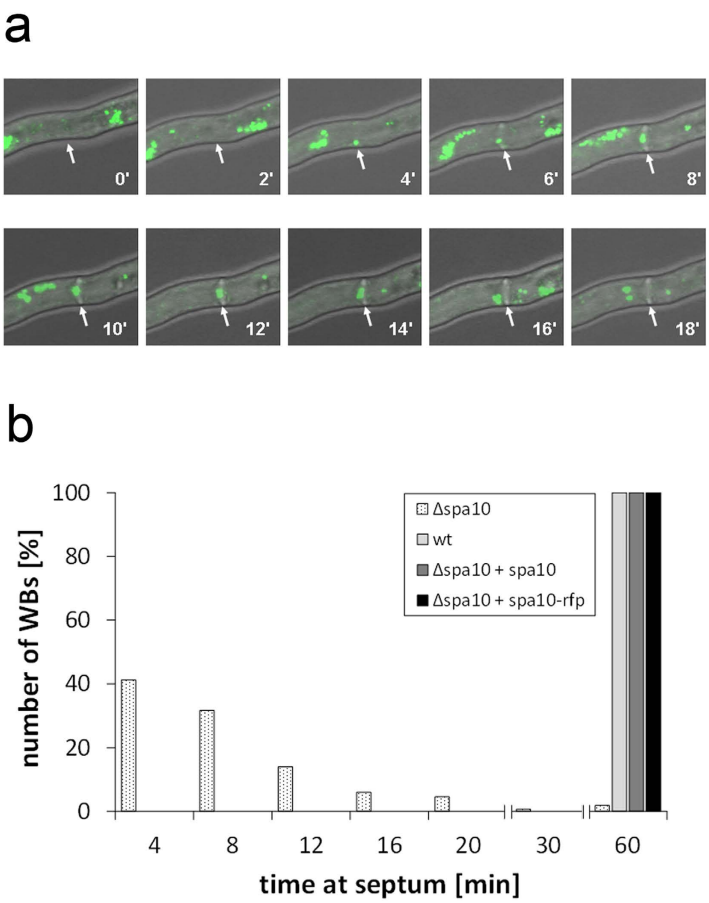


**Figure 7. In the absence of Spa10, Woronin bodies are not or only transiently tethered to the septum.** The micrographs in panel (a) show a hypha of the Δ*spa*10 mutant expressing GFP-HexA. The position of an emerging septum is indicated by arrows. Images represent projections of stacks of confocal images that were taken every 2 min as indicated. Panel (b) shows a quantification of the time Woronin bodies remained at the septal pore. These data derived from live cell imaging of the indicated strains (30 septa per strain).

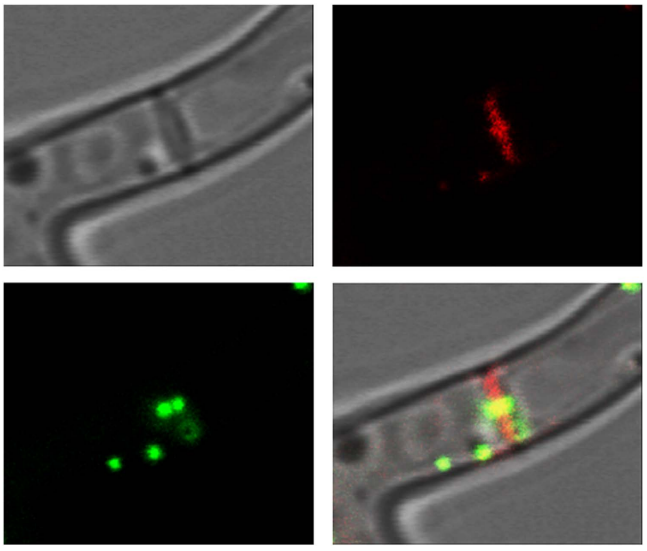

**Figure 8. Complementation of the Δ*spa*10 mutant by expression of Spa10-RFP.** The localization of Spa10-RFP and Woronin bodies tagged with GFP-HexA is shown in red and green, respectively.

## Discussion

The precise positioning of a protein usually requires a specific interaction with a binding partner that is often part of a larger structural framework. Protein domains usually mediate these interactions and represent key elements of the positioning machinery. The Lah protein tethers Woronin bodies at the septum and its C-terminal domain is specifically targeted to the rim of the septal pore[5]. In this study, we have defined a minimal binding domain of 288 aa that is well conserved in different *Aspergillus* Lah proteins and *N. crassa* LAH-2. A coiled-coil domain, predicted for positions 512 to 685 of $LahC_{1000}$, is not required for the targeting to the septal pore. It may, however, be involved in protein-protein interactions between individual Lah proteins, which have been described for *A. fumigatus* and *A. oryzae*[5,11]. In the targeting domain, a transmembrane region is predicted with high probability that divides $LahC_{288}$ in a small intracellular part of 49 aa and a larger extracellular domain of 219 residues. In a septum-bound Lah protein the latter domain would extend into the extracellular space that is formed by the cytoplasmic membrane, which encloses the septal cross-wall. A GFP fusion comprising only the extracellular domain showed no distinct localisation demonstrating that the putative transmembrane region is required for the interaction with the unknown binding partner of Lah at the septum.

A GFP fusion comprising the putative transmembrane region and very short stretches of flanking residues ($LahC_{TM}$) showed a distinct localization, but not at the septal pore. Instead it was enriched in the membrane of round organelle-like structures that enclose nuclei. The localization of $LahC_{TM}$ is very similar to that observed for the *A. fumigatus* NCE102 homologue, which resides in the Endoplasmatic Reticulum[16]. We therefore assume that $LahC_{TM}$ is recruited to the nuclear domain of the Endoplasmatic Reticulum[17]. We initially expected Lah to be a solely cytoplasmic linker between Woronin bodies and the rim of the septal pore. The predicted transmembrane region and the localization of $LahC_{TM}$ challenged this notion. Two lines of evidence furthermore suggest that the C-terminal domain of Lah harbors a trans-membrane region, which is essential for the function of LahC: (i) in protein extracts separated by ultracentrifugation. LahC is found in the pellet fraction and (ii) elimination of the predicted transmembrane region by introduction of point mutations abrogates the targeting of LahC to the septal pore.

It was shown previously that the vegetative hyphae of an *A. fumigatus* Δ*rho4* mutant contains no or only very few septa[14]. In non-septate hyphae, we expected GFP-$LahC_{288}$ to be diffusively distributed in the cytoplasmic membrane. Surprisingly, it showed a clearly distinct localization pattern and was targeted to distinct spot-like structures in or at the cytoplasmic membrane. Live cell analysis revealed a minor lateral mobility for these structures. We assume that these spots represent protein complexes consisting of components of the early septation machinery. They assemble in a Rho4-independent manner, but at a later stage, when Rho4 activity becomes indispensable, the septation process comes to a halt in the Δ*rho4* mutant. Si *et al.*[18] have shown for *A. nidulans* that Rho4 is required for the formation of the contractile actin ring (CAR). We therefore compared the temporal recruitment of LahC and actin using a strain that co-expresses GFP-LahC and LifeAct-RFP and observed an approximately simultaneous recruitment. Thus, Rho4 may control the assembly of the CAR, but not the simultaneous recruitment of LahC. It was an unexpected finding that LahC is already recruited at such an early step of the septation process. However, additional data confirmed that Lah proteins are recruited at this stage, since we observed Woronin bodies that are apparently tethered to nascent septa. According to our current knowledge, it is unlikely that Woronin bodies are directly involved in the septation process, and we therefore assume that the putative LahC receptor represents an essential constituent of the nascent septum, which most likely serves other functions apart from Lah binding.

It is remarkable that the LahC-recruiting spot-like structures persist in the cytoplasmic membrane of the *rho*4 mutant for longer times. Their ability to bind substantial amounts of LahC suggested that some Woronin bodies may be linked to the lateral cell wall of this mutant. Indeed we observed Woronin bodies at this position and thus in a pattern similar to that found in *N. crassa*.

At this stage, we assumed that the receptor of LahC is recruited early during septation and resides permanently at the mature septal pore. Moreover, we hypothesized that it is a membrane protein with an extracellular domain that interacts with the extracellular domain of LahC. Potential candidates might be found in the Spa-family of septal pore-associated proteins[19]. Some of them have already been analysed in *A. nidulans*[15]. Based on these localization data and predictions of transmembrane regions, Spa10 appeared to be a particular promising candidate. A Spa10-RFP fusion expressed in *A. fumigatus* was indeed found to be targeted to the septum. During septum formation, Spa10-RFP appears later than LahC, at a stage when a cross-wall is already visible. Moreover, in comparison to LahC, Spa10-RFP seems to be less focussed at the centre of the septal cross-wall. It was additionally detectable in the cytoplasmic membrane of *A. fumigatus*, a localization that is particularly prominent in conidial bodies and that was never observed for LahC. Thus, there is a clear difference in the temporal and spatial patterns of LahC and Spa10-RFP, which argues against a direct interaction of these proteins. In order to investigate the role of Spa10 in the process of septation, we deleted the corresponding gene. The Δ*spa*10 mutant showed no dramatic defects in growth, colony morphology or sporulation. However, targeting of GFP-$LahC_{288}$ to the mature septum was nearly completely abolished in this mutant and only rarely we observed very weak spots of GFP-$LahC_{288}$ in the centre of septal cross-walls. However, during septum formation the situation was strikingly different. At this stage, GFP-$LahC_{288}$ was strongly recruited; it formed a large ring that constricted parallel to the centripetal growth of the cross wall. At the mature septum, GFP-$LahC_{288}$ signals gradually disappeared and the mutant showed a severe defect in the anchoring of Woronin bodies at the septal pore. In conclusion, these data indicate that Spa10 is not required for the initial recruitment of LahC during septum formation, but it is essential for a stable localization of LahC at the septal pore.

In the Δ*rho*4 mutant, Spa10-RFP is apparently not recruited to the GFP-$LahC_{288}$-containing spots. If these structures are indeed remnants of halted septation events, they should contain only those proteins that are recruited in the early steps of the septation process. The absence of Spa10-RFP demonstrates that Spa10 is

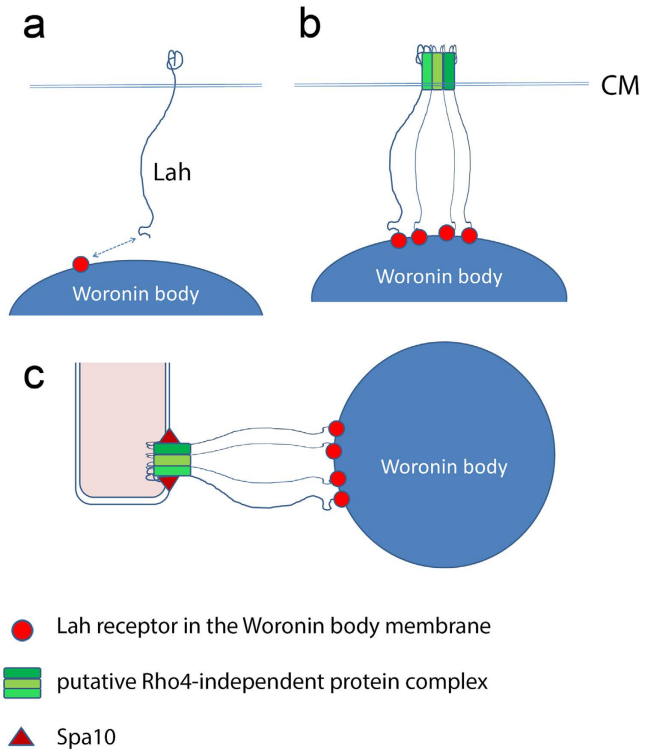


**Figure 9. Hypothetical model of the events leading to the recruitment of Lah and Woronin bodies during septum formation.** (**a**) Lah is a transmembrane protein which resides with its C-terminal part in the cytoplasmic membrane. As long as this protein is diffusely spread in the membrane, its interactions with Woronin bodies are most likely weak and transient. (**b**) We propose that very early during the septation process a putative protein complex assembles in a Rho4-independent manner and recruits Lah proteins via their C-terminal domains. At this stage, Woronin bodies may already be tethered by bundles of Lah proteins. (**c**) In the mature septum, Spa10 is required for a stable anchoring of Woronin bodies. We assume that Spa10 stabilizes the already formed LahC-recruiting protein complex and thereby enables a stable positioning of Woronin bodies.

recruited at a later stage and in a Rho4-dependent manner. Since Spa10 is dispensable for the early recruitment of LahC, we assume that a so far unknown protein or protein complex attracts LahC to the site of septation.

In conclusion, this study provides new insights in the architecture and function of Lah. We show that the C-terminal 288 amino acids are sufficient to recruit Lah to the septum. Our data suggest a sequence of events that is depicted in Fig. 9. Newly formed Lah molecules insert with their C-terminal part in the cytoplasmic membrane, while their N-termini are free to interact with their receptor on the Woronin body surface (Fig. 9a). Given that the anchoring of a Woronin body requires a tethering by many Lah molecules, it is likely that interactions mediated by single or only few Lah molecules are weak and only transient. Thus, at this stage the Lah molecules, which are dispersed in the cytoplasmic membrane, are most likely unable to tether Woronin bodies. When the septation process starts, an early protein complex assembles in a Rho4-independent manner that efficiently recruits Lah. This allows multiple interactions involving many Lah proteins, which already enable an early tethering of Woronin bodies (Fig. 9b). Interestingly, this stage seems to be somehow conserved in the lateral spot-like structures found in the Δ*rho*4 mutant. When the mature septal cross wall is finally formed, a stable localization of LahC at the septal pore requires Spa10 (Fig. 9c). Spa10 may either directly interact with LahC or, more likely, it is stabilizing a larger protein complex that interacts with LahC. In any case, our study identifies Spa10 as the first molecule that is essentially required for a stable positioning of Woronin bodies at the septal pore. To achieve a stable anchoring of a Woronin body at a defined position of the cell envelope, interactions with components of the cell wall are most likely required. Thus, protein complexes may exist in the cytoplasmic membrane that provide docking sites for the two types of leashins and additionally interact with the cell wall. The Spa10 protein may be a first component of such a putative protein complex, but further research is clearly required to define these structures in more detail.

## Methods

**Strains and media.** The *A. fumigatus* strain AfS35 is a derivative of strain D141 lacking the homologous end-joining component AkuA and the Δrho4 mutant have been described previously[14,20]. Aspergillus minimal medium (AMM) was prepared and resting conidia were isolated as described in[5,21] respectively.

| Designation | Sequence | Restriction site |
|---|---|---|
| LahC1044-fwd | GCG**TGTACA**GCCATTGCAGAGTTCGACGAG | Bsp1407I |
| LahC509-fwd | GA**TGTACA**GAGGGATGGGGGGAGTCGCCC | Bsp1407I |
| LahC288-fwd | GA**TGTACA**TTCTCCAAACACTCCGACCAT | Bsp1407I |
| LahC219-fwd | GA**TGTACA**ATGGATCGTGAGCAACGCCAA | Bsp1407I |
| LahC-TM-rev | GAGATATCCTACTTGAGCTTTTGGCGTTGCTC | |
| LahC-rev | TCAGATCACGTTGCTGATATCCATGGTCGA | |
| LahC-mutation | ATATCTTCATGTCCG<u>A</u>GG<u>A</u>GATGACTATGGTGTG | |
| Spa10-fwd | ATGGGTGTCGACACCCGCAGG | |
| Spa10-rev | CGATGGTCGTGTTCAACGTCAACCTGGTC | |
| Spa10-stop-rev | TCAATGGTCGTGTTCAACGTCAA | |
| Δspa10-5′-fwd | ATCAACACTAGGTTAACTAGCTAGC | |
| Δspa10-5′-rev | CG**GGCCATCTAGGCC**CTCGGTAGGAACCAGTGTG | SfiI |
| Δspa10-3′-fwd | GT**GGCCTGAGTGGCC**TCGGTTGTCACGCAACATC | SfiI |
| Δspa10-3′-rev | CTACCCTGTTGGAGGGAGAT | |
| Δspa10-5′-cast | TCTGGGTTGCTGGTCCTCC | |
| Δspa10-3′-cast | GGATTGGCTTCACTGGCAATGTTAG | |
| gpdA(p)-3-rev | TGTCTGCTCAAGCGGGGTAG | |
| XylP-rev | AAACGTTGGTTCTTCGAGTCGATGAATG | |
| gpdA(p)-3-seq-fwd | ACTCCATCCTTCCCATCCC | |
| seq-mRFP1-rev | TTCACGGAGCCCTCCATG | |

**Table 1. Oligonucleotides used in this study.**

**Sequence analysis and data base searches.** Sequences from different Aspergillus species were obtained from the Aspergillus genome database (AspGD; http://www.aspergillusgenome.org/). Homology searches were performed using BlastP at Fungal Genomes Central - NCBI - NIH (http://www.ncbi.nlm.nih.gov/projects/genome/guide/fungi/). For sequence alignments we used Clustal Omega (http://www.ebi.ac.uk/Tools/msa/clustalo/). Transmembrane regions were predicted using TMpred (http://www.ch.embnet.org/software/TMPRED_form.html) or PHOBIUS (http://phobius.sbc.su.se/). Further analysis of protein sequences was performed using SMART (http://smart.embl.de/) and 2ZIP - Server (http://2zip.molgen.mpg.de/cgi-bin/2zip.pl).

**Construction of strains expressing fluorescent fusion proteins.** The LifeAct-RFP plasmid was a kind gift of Dr. W.J. Steinbach (Duke University Medical Center, Durham, NC, USA)[22]. The GFP-HexA, GFP-LahC$_{1000}$ and LahN-GFP constructs have been described previously[5,23].

To generate the different truncated LahC derivatives schematically depicted in Figs 2 and 3, suitable fragments were amplified by PCR using the Q5 high fidelity polymerase (New England Biolabs) and the oligonucleotides given in Table 1. The resulting blunt end PCR products were subsequently cloned into the EcoRV site of pSK379s-GFP. To generate the Spa10-RFP construct, the *spa10* sequence was amplified by PCR (without STOP codon) and cloned into the PmeI site of pSK379mRFP. To generate the complementation construct, the *spa10* sequence was amplified by PCR using primer combination Spa10-fwd/Spa10-stop-rev and cloned into the PmeI site of pSK379. All construct were sequenced before transformation.

**Generation of point mutations.** The transmembrane region at the C terminus of Lah was mutated using the Change-IT™ Multiple Mutation Site Directed Mutagenesis Kit (Affymetrix) and the oligonucleotide 'LahC-mutation' according to the instructions of the vendor. The mutations were verified by sequencing.

**Analysis of protein extracts.** Aspergillus minimal medium (AMM) was inoculated with conidia of *A. fumigatus* AfS35 strain expressing GFP-LahC$_{TM}$ and the culture was incubated with shaking at 37 °C for 16 h. The resulting mycelium was harvested and washed in 10 mM HEPES buffer (pH 7.4). The pellet was resuspended in HEPES buffer and a lysate was generated using a FastPrep24 (MP Biomedicals). The extract was cleared by centrifugation (15 min, 10,000 g) and subsequently fractionated by ultracentrifugation (100,000 g for 60 min). Samples representing similar fractions of the initial extract were separated by SDS-PAGE electrophoresis and blotted onto a nitrocellulose membrane. The blot was finally developed using a rabbit anti-GFP antibody and a suitable peroxidase-labeled secondary antibody.

**Microscopy and live cell imaging.** To analyse fluorescent fusion proteins, conidia of the respective strains were inoculated in 8-well ibidi-chambers or 60 μ-dishes (ibidi GmbH, Martinsried, Germany) containing AMM. Germ tubes were generated by overnight incubation at 30 °C. Fungal cells were then grown to the desired length and the samples were analysed using a Leica SP-5 microscope equipped with an environmental chamber adjusted to 37 °C (Leica Microsystems). To analyse fluorescent fusion proteins, conidia of the respective strains were inoculated in 8-well ibidi-chambers or 60 μ-dishes (ibidi GmbH) containing AMM. When the hyphae reached an appropriate length, they were analysed using a Leica SP-5 microscope equipped with an environmental chamber

adjusted to 37 °C (Leica Microsystems, Wetzlar, Germay). All micrographs were taken using a Leica HCX PL APO lamda blue 63 × 1.4 Oil UV objective. Further image processing was performed using Adobe Photoshop CS. Time-lapse confocal images were recorded using a Leica SP-5 microscope under the conditions described above. The resulting image stacks were merged and exported as avi files using the SP-5 and ImageJ software. To quantify the time that a Woronin body remained at a certain septum, strains expressing GFP-HexA were analysed by live cell imaging. 30 septa per strain were analysed by generating image stacks every 2 min over a period of 1 h.

**Construction of the Δspa10 mutant strain.** All oligonucleotides used to generate the deletion and complementation constructs are listed in Table 1. For cloning experiments, PCR reactions were performed using the Q5 high fidelity polymerase (New England Biolabs). To construct a suitable replacement cassette, a 3.5 kb hygromycin resistance cassette was excised from pSK346 using SfiI. 1000 bp upstream and downstream of the *spa*10 gene (Afu4g13320) were amplified by PCR from chromosomal DNA using the oligonucleotide pairs Δspa10-5′-fwd/Δspa-5′-rev and Δspa-3′-fwd/Δspa-3′-rev. After digestion with SfiI the PCR products were ligated to the hygromycin cassette. The resulting deletion construct was transformed into protoplast of *A. fumigatus* strain AfS35 and the cells were then transferred to AMM plates containing 1.2 M sorbitol and either 200 μg/ml hygromycin (Roche, Applied Science, Mannheim, Germany). To verify the mutant, we amplified *spa*10 using oligonucleotides spa10-fwd/spa10-rev (PCR1). The inserted hygromycin cassette was detected using the primer combinations Δspa10-5′-cast/gpdA(p)-3-rev (PCR2) and hph-3-SmaI/Δspa10-3′-cast (PCR3). The complementation of the mutant with *spa*10 and *spa*10-*rfp* was verified using the primer combinations gpdA(p)-3-seq-fwd/Spa10-rev and gpdA(p)-3-seq-fwd/seq-mRFP1-rev.

**Phenotypic plate assays.** Isolated conidia were counted using a Neubauer chamber. For drop dilution assays, a series of ten-fold dilutions starting with $5 \times 10^7$ conidia/ml were spotted onto AMM plates in aliquots of 3 μl; if indicated, plates were supplemented with 25 μg/ml Calcofluor white and incubated at 37 °C.

## References


1. Ng, S. K., Liu, F., Lai, J., Low, W. & Jedd, G. A tether for Woronin body inheritance is associated with evolutionary variation in organelle positioning. *PLoS Genet* **5,** e1000521 (2009).
2. Markham, P. & Collinge, A. J. Woronin bodies of filamentous fungi. *FEMS Microbiol Rev* **46,** 1–11 (1987).
3. Soundararajana, S. *et al.* Woronin body function in *Magnaporthe grisea* is essential for efficient pathogenesis and for survival during nitrogen starvation stress. *Plant Cell* **16,** 1564–1574 (2004).
4. Liang, L. *et al.* The Woronin body in the nematophagous fungus *Arthrobotrys oligospora* is essential for trap formation and efficient pathogenesis. *Fungal Biol* **121,** 11–20 (2017).
5. Beck, J., Echtenacher, B. & Ebel, F. Woronin bodies, their impact on stress resistance and virulence of the pathogenic mould *Aspergillus fumigatus* and their anchoring at the septal pore of filamentous Ascomycota. *Mol Microbiol* **89,** 857–871 (2013).
6. Dichtl, K. *et al. Aspergillus fumigatus* devoid of cell wall β-1,3-glucan is viable, massively sheds galactomannan and is killed by septum formation inhibitors. *Mol Microbiol* **95,** 458–471 (2015).
7. Jedd, G. Fungal evo-devo: organelles and multicellular complexity. *Trends Cell Biol* **21,** 12–19 (2011).
8. Jedd, G. & Chua, N. H. A new self-assembled peroxisomal vesicle required for efficient resealing of the plasma membrane. *Nat Cell Biol* **2,** 226–231 (2000).
9. Leonhardt, Y., Beck, J. & Ebel, F. Functional characterization of the Woronin body protein WscA of the pathogenic mold *Aspergillus fumigatus*. *Int J Med Microbiol* **306,** 165–173 (2016).
10. Plamann, M. Cytoplasmic streaming in Neurospora: disperse the plug to increase the flow? *PLoS Genet* **5,** e1000526 (2009).
11. Han, P., Jin, F. J., Maruyama, J. & Kitamoto, K. A large nonconserved region of the tethering protein Leashin is involved in regulating the position, movement, and function of Woronin bodies in *Aspergillus oryzae*. *Eukaryot Cell* **13,** 866–877 (2014).
12. Egan, M. J., McClintock, M. A. & Reck-Peterson, S. L. Microtubule-based transport in filamentous fungi. *Curr Opin Microbiol* **15,** 637–645 (2012).
13. Isermann, P. & Lammerding, J. Nuclear mechanics and mechanotransduction in health and disease. *Curr Biol* **23,** R1113–21 (2013).
14. Dichtl, K., Helmschrott, C., Dirr, F. & Wagener, J. Deciphering cell wall integrity signalling in *Aspergillus fumigatus*: identification and functional characterization of cell wall stress sensors and relevant Rho GTPases. *Mol Microbiol* **83,** 506–519 (2012).
15. Shen, K. F., Osmani, A. H., Govindaraghavan, M. & Osmani, S. A. Mitotic regulation of fungal cell-to-cell connectivity through septal pores involves the NIMA kinase. *Mol Biol Cell* **25,** 763–775 (2014).
16. Khalaj, V., Azizi, M., Enayati, S., Khorasanizadeh, D. & Ardakani, E. M. NCE102 homologue in *Aspergillus fumigatus* is required for normal sporulation, not hyphal growth or pathogenesis. *FEMS Microbiol Lett* **329,** 138–45 (2012).
17. Maruyama, J. & Kitamoto, K. Differential distribution of the endoplasmic reticulum network in filamentous fungi. *FEMS Microbiol Lett* **272,** 1–7 (2007).
18. Si, H., Justa-Schuch, D., Seiler, S. & Harris, S. D. Regulation of septum formation by the Bud3-Rho4 GTPase module in *Aspergillus nidulans*. *Genetics* **185,** 165–176 (2010).
19. Lai, J. *et al.* Intrinsically disordered proteins aggregate at fungal cell-to-cell channels and regulate intercellular connectivity. *Proc Natl Acad Sci USA* **109,** 15781–15786 (2012).
20. Krappmann, S., Sasse, C. & Braus, G. H. Gene targeting in *Aspergillus fumigatus* by homologous recombination is facilitated in a nonhomologous end- joining-deficient genetic background. *Eukaryot Cell* **5,** 212–215 (2006).
21. Rohde, M., Schwienbacher, M., Nikolaus, T., Heesemann, J. & Ebel, F. Detection of early phase specific surface appendages during germination of *Aspergillus fumigatus* conidia. *FEMS Microbiol Lett* **206,** 99–105 (2002).
22. Juvvadi, P. R. *et al.* Localization and activity of the calcineurin catalytic and regulatory subunit complex at the septum is essential for hyphal elongation and proper septation in *Aspergillus fumigatus*. *Mol Microbiol* **82,** 1235–1259 (2011).
23. Beck, J. & Ebel, F. Characterization of the major Woronin body protein HexA of the human pathogenic mold *Aspergillus fumigatus*. *Int J Med Microbiol* **303,** 90–97 (2013).


## Acknowledgements

We thank Kirsten Niebuhr-Ebel for critical reading of the manuscript and William J. Steinbach for the LifeAct-RFP plasmid. This work was funded by the FoeFoLe-program of the Medical Faculty of the Ludwig-Maximilians-University.

## Author Contributions

Y.L. and S.C.K. performed the experiments and provided graphics. F.E. designed the experiments and wrote the manuscript. J.W. provided reagents.

## Additional Information

**Supplementary information** accompanies this paper at http://www.nature.com/srep

**Competing Interests:** The authors declare no competing financial interests.

**How to cite this article:** Leonhardt, Y. *et al.* Lah is a transmembrane protein and requires Spa10 for stable positioning of Woronin bodies at the septal pore of *Aspergillus fumigatus*. *Sci. Rep.* **7**, 44179; doi: 10.1038/srep44179 (2017).

# Literatur


Aruanno, M., Glampedakis, E., and Lamoth, F. (2019). Echinocandins for the treatment of invasive aspergillosis: from laboratory to bedside. *Antimicrobial Agents and Chemotherapy*, 63(8):e00399-19.

Beck, J. and Ebel, F. (2013). Characterization of the major woronin body protein hexa of the human pathogenic mold aspergillus fumigatus. *International Journal Of Medical Microbiology*, 303:90–97.

Beck, J., Echtenacher, B., and Ebel, F. (2013). Woronin bodies, their impact on stress resistance and virulence of the pathogenic mould aspergillus fumigatus and their anchoring at the septal pore of filamentous ascomycota. *Molecular Microbiology*, 89:857–871.

Berns, M. W., Aist, J. R., Wright, W. H., and Liang, H. (1992). Optical trapping in animal and fungal cells using a tunable, near-infrared titanium-sapphire laser. *Experimental Cell Research*, 198(2):375–378.

Bleichrodt, R., Veluw, G., Recter, B., Maruyama, J., Kitamoto, K., and Wösten, H. (2012). Hyphal heterogeneity is maintained by septal closure. *Molecular Microbiology*, 86:1334–1344.

Collinge, A. and Markham, P. (1985). Woronin bodies rapidly plug septal pores of severed penicillium chrysogenum hyphae. *Experimental Mycology*, 9:80–85.

Dagenais, T. R. T. and Keller, N. P. (2009). Pathogenesis of aspergillus fumigatus in invasive aspergillosis. *Clinical Microbiology Reviews*, 22(3):447–465.

Dichtl, K., Helmschrott, C., Dirr, F., and Wagener, J. (2012). Deciphering cell wall integrity signalling in aspergillus fumigatus: identification and functional characterization of cell wall stress sensors and relevant rho gtpases. *Molecular Microbiology*, 83(3):506–519.

Dichtl, K., Samantaray, S., Aimanianda, V., Zhu, Z., Prévost, M.-C., Latgé, J.-P., Ebel, F., and Wagener, J. (2015). Aspergillus fumigatus devoid of cell wall beta-1,3-glucan is viable, massively sheds galactomannan and is killed by septum formation inhibitors. *Molecular Microbiology*, 95(3):458–471.

Fang, W. and Latgé, J.-P. (2018). Microbe profile: Aspergillus fumigatus: a saprotrophic and opportunistic fungal pathogen. *Mircrobiology*, 164(8):1009–1011.

Garrison, R. G., Lane, J. W., and Field, M. F. (1970). Ultrastructural changes during the yeastlike to mycelial-phase conversion of blastomyces dermatitidis and histoplasma capsulatum. *Journal of bacteriology*, 101(2):628–635.

Jedd, G. and Chua, N. H. (2000). A new self-assembled peroxisomal vesicle required for efficient resealing of the plasma membrane. *Nat Cell Biol*, 2(4):226–231.

Jumar, R., Chugh, T., and Gaur, S. N. (2003). Allergic bronchopulmonary aspergillosis - a review. *Indian J Allergy Astma Immunol*, 17(2):55–66.

Kawamura, S., Maesaki, S., Tomono, K., Tashiro, T., and Kohno, S. (2000). Clinical evaluation of 61 patients with pulmonary aspergilloma. *Internal Medicine*, 39(3):209–212.

Kwon-Chung, K. J. and Sugui, J. A. (2013). Aspergillus fumigatus – what makes the species a ubiquitous human fungal pathogen? *PLOS Pathogens*, 9(12):1–4.

Lai, J., Koh, C. H., Tjota, M., Pieuchot, L., Raman, V., Chandrababu, K. B., Yang, D., Wong, L., and Jedd, G. (2012). Intrinsically disordered proteins aggregate at fungal cell-to-cell channels and regulate intercellular connectivity. *Proc Natl Acad Sci U S A*, 109(39):15781–15786.

Latgé, J.-P. (1999). Aspergillus fumigatus and aspergillosis. *Clinical Microbiology Reviews*, 12(2):310–350.

Leonhardt, Y., Beck, J., and Ebel, F. (2016). Functional Characterization of the Woronin body protein WscA of the pathogenic mold Aspergillus fumigatus. *International Journal Of Medical Microbiology*, 306, 165-173.

Liang, L., Gao, H., Li, J., Liu, L., Liu, Z., and Zhang, K.-Q. (2017). The woronin body in the nematophagous fungus arthrobotrys oligospora is essential for trap formation and efficient pathogenesis. *Fungal Biology*, 121(1):11–20.

Lin, S.-J., Schranz, J., and Teutsch, S. M. (2001). Aspergillosis case-fatality rate: Systematic review of the literature. *Clinical Infectious Diseases*, 32(3):358–366.

Liu, F., Ng, S. K., Lu, Y., Low, W., Lai, J., and Jedd, G. (2008). Making two organelles from one: Woronin body biogenesis by peroxisomal protein sorting. *J Cell Biol*, 180(2):325–339.

Markham, P. and Collinge, A. (1987). Woronin bodies of filamentous fungi. *FEMS Microbiology Letters*, 46:1–11.

McCormick, A., Loeffler, J., and Ebel, F. (2010). Aspergillus fumigatus: contours of an opportuistic human pathogen. *Cellular Microbiology*, 12(11):1535–1543.

Momany, M., Richardson, E. A., Van Sickle, C., and Jedd, G. (2002). Mapping woronin body position in aspergillus nidulans. *Mycologia*, 94(2):260–266.

Ng, S. K., Liu, F., Lai, J., Low, W., and Jedd, G. (2009). A tether for woronin body inheritance is associated with evolutionary variation in organelle positioning. *PLoS Genet*, 5(6):e1000521.

Raveendran, S. and Lu, Z. (2018). Ct findings and differential diagnosis in adults with invasive pulmonary aspergillosis. *Radiology of Infectious Diseases*, 5(1):14 – 25.

Shatkin, A. and Tatum, E. (1959). Electron microscopy of neurospora crassa mycelia. *J Biophys Biochem Cytol*, 6(3):423–426.

Shen, K.-F., Osmani, A. H., Govindaraghavan, M., and Osmani, S. A. (2014). Mitotic regulation of fungal cell-to-cell connectivity through septal pores involves the nima kinase. *Mol Biol Cell*, 25(6):763–775.

Soundararajan, S., Jedd, G., Li, X., Ramos-Pamploña, M., Chua, N. H., and Naqvi, N. I. (2004). Woronin body function in magnaporthe grisea is essential for efficient pathogenesis and for survival during nitrogen starvation stress. *The Plant cell*, 16(6):1564–1574.

Tenney, K., Hunt, I., Sweigard, J., Pounder, J. I., McClain, C., Bowman, E. J., and Bowman, B. J. (2000). hex-1, a gene unique to filamentous fungi, encodes the major protein of the woronin body and functions as a plug for septal pores. *Fungal Genetics and Biology*, 31(3):205–217.

Trinci, A. P. J. and Collinge, A. J. (1974). Occlusion of the septal pores of damaged hyphae of neurospora crassa by hexagonal crystals. *Protoplasma*, 80(1):57–67.

Ullmann, A. J., Aguado, J. M., Arikan-Akdagli, S., Denning, D. W., Groll, A. H., Lagrou, K., Lass-Flörl, C., Lewis, R. E., Munoz, P., Verweij, P. E., Warris, A., Ader, F., Akova, M., Arendrup, M. C., Barnes, R. A., Beigelman-Aubry, C., Blot, S., Bouza, E., Brüggemann, R. J. M., Buchheidt, D., Cadranel, J., Castagnola, E., Chakrabarti, A., Cuenca-Estrella, M., Dimopoulos, G., Fortun, J., Gangneux, J. P., Garbino, J., Heinz, W. J., Herbrecht, R., Heussel, C. P., Kibbler, C. C., Klimko, N., Kullberg, B. J., Lange, C., Lehrnbecher, T., Löffler, J., Lortholary, O., Maertens, J., Marchetti, O., Meis, J. F., Pagano, L., Ribaud, P., Richardson, M., Roilides, E., Ruhnke, M., Sanguinetti, M., Sheppard, D. C., Sinkó, J., Skiada, A., Vehreschild, M. J. G. T., Viscoli, C., and Cornely, O. A. (2018). Diagnosis and management of aspergillus diseases: executive summary of the 2017 escmid-ecmm-ers guideline. *Clinical Microbiology and Infection*, 24:e1–e38.

World Health Organization (2018). Global health estimates 2016: Deaths by cause, age, sex, by country and by region, 2000-2016. *Geneva*.

Woronin, M. (1864). Entwicklungsgeschichte des *Ascobolus pucherrimus* cr. und einiger pezizen. *Abh Senkenb Naturforsch*, 5(344-355).

Zheng, S., Li, X., Hu, B., and Li, H. (2018). Is adjuvant antifungal therapy after video-assisted thoracic surgery for pulmonary aspergilloma necessary? *J Thorac Dis*, 10(11):6060–6065.

# Danksagung

Der größte Dank gebührt Herrn Prof. Dr. Frank Ebel, der mit viel Geduld und großem Enthusiasmus in Theorie und Praxis diese Arbeit betreut hat und zu jedem Zeitpunkt während meiner Zeit im Labor für große wie kleine Probleme stets ein offenes Ohr hatte.

Mein besonderer Dank gilt auch allen Labormitgliedern der AG Ebel und AG Wagener des Max von Pettenkofer-Instituts für die arbeitsbezogenen sowie -fernen Gespräche und die Freundschaften, die hier entstanden sind: Dominik Ruf, Veronika Loiko, Johannes Wagener, Victor Brantl, Sara Kakoschke, Tamara Kakoschke, Berna Bonanza, Mirjam Penka, Anja Spadinger, Laura Sturm, Annegret Vaggelas und Karl Dichtl. Danke für die einzigartige, tolle Zeit.

Zu guter Letzt sei meiner Familie gedankt für die geduldige Unterstützung über das Studium und meine Promotionszeit hinweg.